A THEORETICAL AND EXPERIMENTAL INVESTIGATION OF TUNNEL DIODE NOISE

A Thesis

Presented to

the Faculty of Graduate Studies and Research

The University of Manitoba

In Partial Fulfillment

of the Requirements for the Degree

Master of Science in Electrical Engineering

---

by

Harry Bernard Wall

February 1965

ACKNOWLEDGMENT

The author wishes to express his sincere thanks to the National Research Council for its financial assistance and to Professor Ernest Bridges of the University of Manitoba for his guidance throughout the project.

ABSTRACT

The junction currents of a tunnel diode and the mechanism producing them are outlined. Noise in electronic components is discussed and a theoretical noise model of the tunnel diode developed. The effects on this model of the parasitic elements present in a physical diode are calculated. Noise measurements using two variations of the substitution method are performed on three General Electric Co. 1N2939 tunnel diodes at a frequency of 30 megacycles per second. The application of the results to the minimum noise figure of tunnel diode amplifiers is discussed.

TABLE OF CONTENTS

CHAPTER		PAGE
I	INTRODUCTION	1
II	TUNNEL DIODE JUNCTION CURRENTS AND THEIR MECHANISM	5
	Esaki and Zener Tunneling Currents	5
	Excess Current	11
	Conventional Diode Forward Current	12
	Reverse Current	13
III	NOISE IN ELECTRONIC COMPONENTS	15
	Noise in Resistors	15
	Thermal noise	15
	Noise bandwidth	18
	Contact noise	19
	Noise in Vacuum Diodes	19
	Shot noise	19
	Flicker noise	21
	Use of a temperature limited vacuum diode as a noise generator	21
	Noise in Semiconductors	23
IV	THEORETICAL TUNNEL DIODE NOISE MODEL	25
	Simplified Equivalent Circuit	25
	Noise Due to Tunneling Currents	26
	Excess Noise in the Valley Region	27
	Noise at Higher Forward Biases	27
	Equivalent Noise Resistance	29

CHAPTER PAGE

V EFFECT OF PARASITIC ELEMENTS ON I_n......... 32
Exact Equivalent Circuit................. 32
Equivalent Noise Circuit................. 34
VI NOISE MEASUREMENTS......................... 38
Wiens Method............................. 38
Tiemann Method........................... 42
Comparison of Wiens and Tiemann Methods.. 44
VII DISCUSSION AND CONCLUSIONS................ 50
Discussion of Results.................... 50
Conclusions.............................. 53
APPENDIXES
A MEASUREMENT OF TUNNEL DIODE PARAMETERS..... 55
Measurement of Diode V-I Characteristic.. 55
Accurate point by point method......... 55
Oscilloscope display of V-I curve...... 56
Measurement of Diode Dynamic Conductance. 61
Measurement of Diode Spreading Resistance 63
Measurement of Diode Junction Capacitance 65
Measurement of Diode Lead Inductance..... 66
B MEASUREMENT OF RECEIVER NOISE FIGURE........ 67
BIBLIOGRAPHY.................................... 71

LIST OF FIGURES

FIGURE		PAGE
1	Tunnel Diode V-I Curve	2
2	Tunnel Diode Energy Band Diagrams	8
3	Tunnel Diode Junction Currents	14
4	Representation of Resistor Thermal Noise	17
5	Equivalent Noise Bandwidth	18
6	Representation of Vacuum Diode Shot Noise	20
7	Circuit Diagram of Noise Generator	22
8	Tunnel Diode Theoretical Equivalent Noise Current	28
9	Tunnel Diode Equivalent Noise Resistance	29
10	Ratio of Tunnel Diode Dynamic to Noise Resistance	30
11	Tunnel Diode Equivalent Circuit	32
12	Tunnel Diode Equivalent Noise Circuit	34
13	Tunnel Diode Shunt Equivalent Noise Circuit	34
14	Effect of Parasitic Elements on I_n	36
15	Test Circuit for Tunnel Diode Noise Measurements at 30 Megacycles	40
16	Comparison of Experimental and Theoretical Equivalent Shot Noise Currents	45
17	Comparison of Experimental and Theoretical Equivalent Shot Noise Currents	46
18	Comparison of Experimental and Theoretical Equivalent Shot Noise Currents	47

FIGURE PAGE

19 Plot of Noise Currents in Wiens Method..... 48

20 Minimum Noise Figure of Tunnel Diode Amplifiers................................. 52

A.1 Circuit for Accurate Measurement of V-I Curve.................................... 55

A.2 Accurate V-I Curve of G.E. 1N2939 Tunnel Diode.................................... 57

A.3 Accurate V-I Curve of G.E. 1N2939 Tunnel Diode.................................... 58

A.4 Accurate V-I Curve of G.E. 1N2939 Tunnel Diode.................................... 59

A.5 Circuit For Displaying Tunnel Diode V-I Curve.................................... 60

A.6 Test Circuit for Measuring Tunnel Diode Dynamic Conductance and Junction Capacitance 62

A.7 Scope Traces in Spreading Resistance Measurement................................ 64

A.8 Receiver Noise Figure...................... 69

LIST OF TABLES

TABLE PAGE

I Tunnel Diode Equivalent Circuit Element Values... 33

CHAPTER I

INTRODUCTION

In 1958, Dr. L. Esaki[1*], a Japanese physicist, published an account of a new phenomenon he discovered in heavily doped (10^{19}atoms/cm^3) p-n junction diodes. The effect of this heavy doping was a V-I characteristic that exhibited a negative dynamic conductance over a range of forward biases. These diodes have come to be called "tunnel diodes", from the quantum mechanical tunneling process that produces their negative conductance. The V-I curve for a General Electric type 1N2939 tunnel diode is shown in Figure 1.

By the quantum mechanical tunneling process, an electron (at the speed of light), can appear to tunnel through a potential barrier that it doesn't have the energy to climb. The conditions necessary for this process to take place are discussed in Chapter II.

Because of the speed at which tunneling takes place, and because of its simple physical construction, the tunnel diode offers many advantages over transistors in such applications as high frequency amplifiers and oscillators. Tunnel diodes are also used in mixers. In these applications a fundamental limitation on the usefulness of the diodes is the amount of noise it produces.

---

*The numeral denotes reference number as listed in bibliography

Figure 1

TUNNEL DIODE V-I CHARACTERISTIC

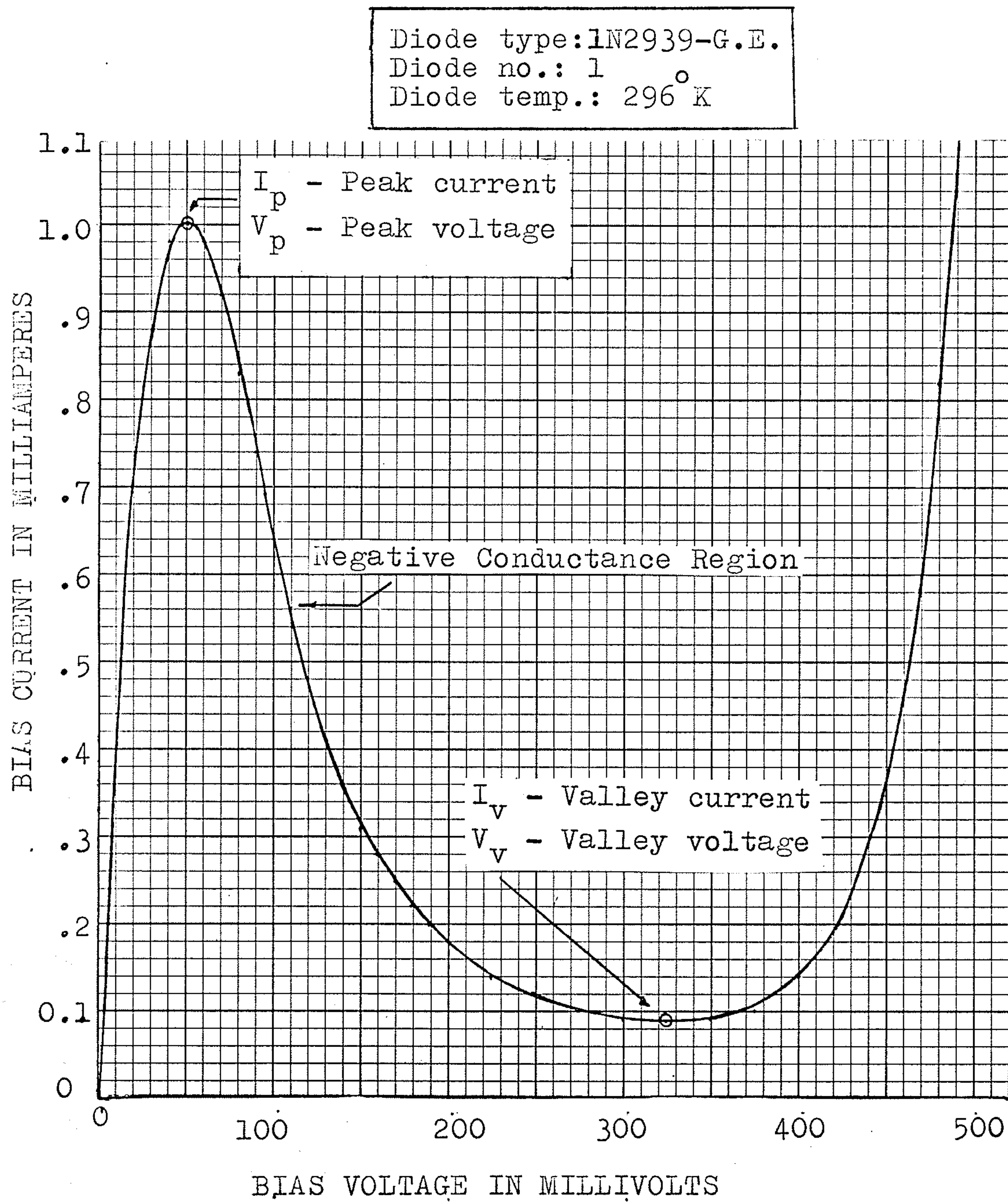

The purpose of this investigation was to study, by theoretical and experimental means, the amount of noise produced by tunnel diodes at a frequency of 30 megacycles. All experimental work was performed on G.E. type 1N2939 tunnel diodes. This diode has a relatively low peak current (1ma), which made it easier to stabilize in the negative conductance region. Some noise measurements had already been performed on this particular type by Wiens[2], and it was hoped this investigation would supplement his previous work.

Noise in tunnel diodes has also been investigated by Chang[3], Tiemann[4], Agourdis and van Vliet[5], and King and Sharpe[6].

To obtain a measure of the noise produced by the tunnel diode, it was compared with the standard noise source of a temperature limited vacuum diode. The plate current required to produce the same amount of noise as the tunnel diode under test is called its "equivalent shot noise current". The noise produced by a tunnel diode was also compared to that of a resistor exhibiting thermal noise.

In Chapter II the different junction currents flowing in a tunnel diode and their producing mechanism are discussed.

In Chapter III the noise produced in electronic components such as resistors, vacuum diodes and semiconductors is outlined.

A theoretical noise model for the tunnel diode is given in Chapter IV. The effect on this model by the diode's parasitic elements is discussed in Chapter V.

The two measurement methods used are outlined in Chapter VI. In Chapter VII the results obtained are discussed and the conclusions arrived at given.

Appendix A gives the techniques used to measure the diode's V-I curve, dynamic conductance, series and spreading resistance, junction capacitance and lead inductance.

Appendix B contains the noise figure measurement of the receiving system used in the noise measurements.

CHAPTER II

TUNNEL DIODE JUNCTION CURRENTS AND THEIR MECHANISM

The net current (I_b) flowing in a tunnel diode is composed of four separate and uncorrelated currents. Each of these currents plays a major role in determining I_b over some particular range of bias voltages. The currents are the Esaki tunneling current (I_E), the Zener tunneling current (I_Z), the excess current (I_x), and the conventional diode forward current (I_f).

The mechanism producing each of the preceeding currents and an expression of their dependence on the bias voltage (V) is discussed in this chapter.

Esaki and Zener Tunneling Currents

The mechanism producing the tunneling currents is dependent on the junction doping densities. This was proven by Hall[7] when he observed the change in the V-I characteristic of a p-n junction with changing doping densities. The minimum doping density required to produce appreciable tunneling is about 10^{19}atoms/cm^3. At doping densities as high as this, several changes are noted in the energy band diagram of the junction.

First the Fermi level is found in the conduction band on the n side and in the valence band on the p side. By definition of the Fermi level, an energy state below the Fermi level has a probability of at least $\frac{1}{2}$ of being occupied. Conversely a state above the Fermi level has a probability of at least $\frac{1}{2}$ of

being unoccupied. Therefore a considerable number of states in the n side conduction band will be filled, while an appreciable number of states at the top of the p side valence band will be empty. Semiconductors, where this occurs, are termed "degenerate".

A second result of high doping densities is that the donor and acceptor states broaden out into bands and cause what is known as "band gap tailing". This effect causes the band gap to narrow considerably. For example, in germanium it causes a decrease of from 0.665ev for the intrinsic case to about 0.5ev for degenerate doping.

The energy band diagram of a degenerate p-n junction at zero bias, showing the two effects is given in Figure 2(a).

The conditions required for quantum mechanical tunneling to occur are given as:

1. Occupied energy states must exist on the side from which the electrons are to tunnel.

2. Unoccupied states must exist at the same energy level as the electrons in condition 1 on the side to which the electrons are to tunnel.

3. The height and width of the potential barrier must be low enough so that the tunneling probability is not negligibly small.

4. Momentum must be conserved in the process.

In the energy band model of the junction at thermal equilibrium (zero bias), as shown in Figure 2(a), these conditions exist to the same degree on both sides of the junction.

This gives rise to two equal but opposite tunneling electron currents. The one flowing from the conduction band on the n side to the valence band on the p side is called the Esaki current (I_E), while the one flowing in the opposite direction is called the Zener current (I_Z).

Esaki[1] has formulated the two currents as :

$$I_E = A\int_{E_{cn}}^{E_{vn}} f_c(E)\rho_c(E)Z_{cv}\left(1-f_v(E)\right)\rho_v(E)dE \quad \ldots\ldots\ldots\ldots 2.1$$

$$I_Z = A\int_{E_{cn}}^{E_{vn}} f_v(E)\rho_v(E)Z_{vc}\left(1-f_c(E)\right)\rho_c(E)dE \quad \ldots\ldots\ldots\ldots 2.2$$

where E is the energy variable, A is a constant depending on the junction area, and Z_{cv} and Z_{vc} are the probabilities of an electron tunneling from the n side conduction band to the p side valence band and visa versa respectively. The variables $f_c(E)$ and $f_v(E)$ are the Fermi-Dirac occupation functions for the conduction and valence band. They are given by the expression:

$$f_{c,v}(E) = \frac{1}{(1 + \exp.(E - E_{fc,v})/kT)} \quad \ldots\ldots\ldots\ldots 2.3$$

where k is Boltzmans constant (1.38×10^{-23} Joules/^{o}K), T is the temperature in degrees K and $E_{fc,v}$ is the Fermi level in the conduction or valence band. $\rho_c(E)$ and $\rho_v(E)$ are the energy level densities in the conduction and valence band respectively.

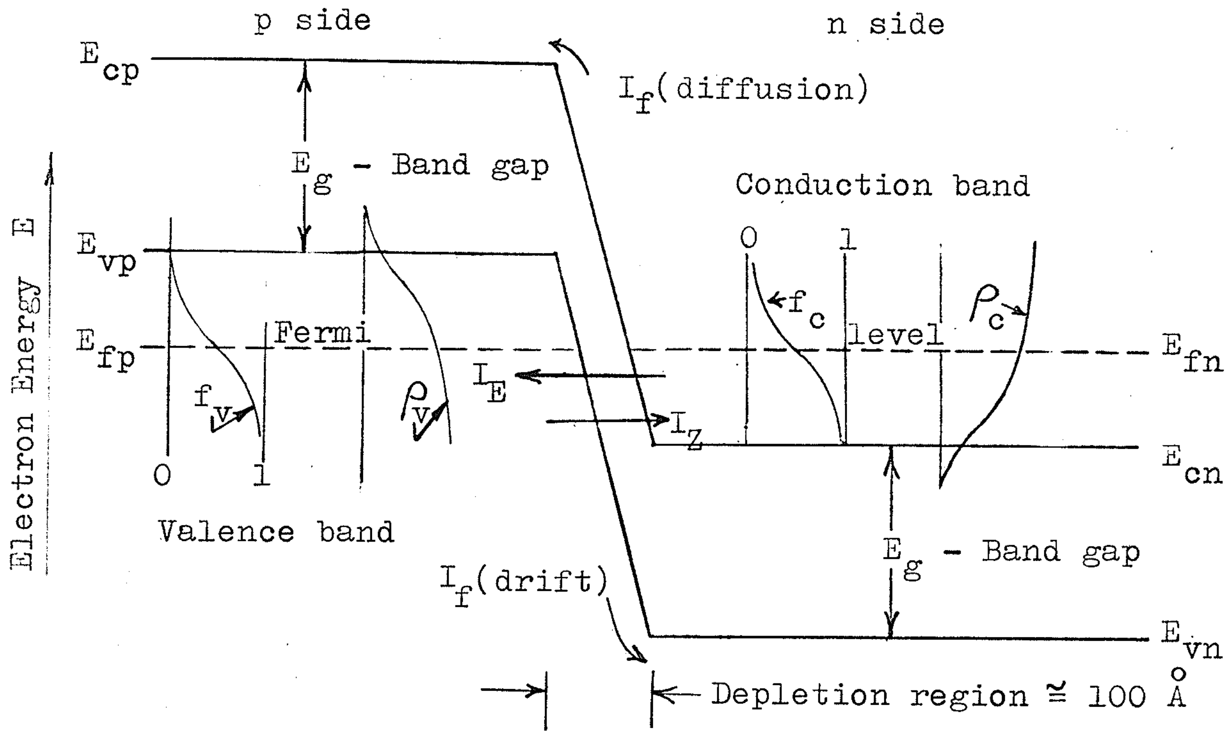

Fig. 2(a) TUNNEL DIODE ENERGY BAND DIAGRAM AT ZERO BIAS

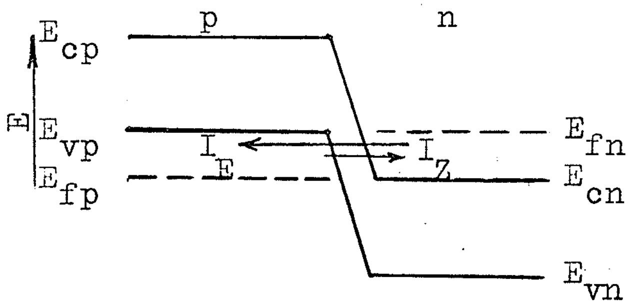

Fig. 2(b) PEAK BIAS

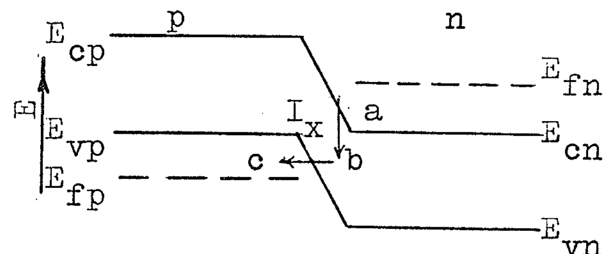

Fig. 2(c) VALLEY BIAS

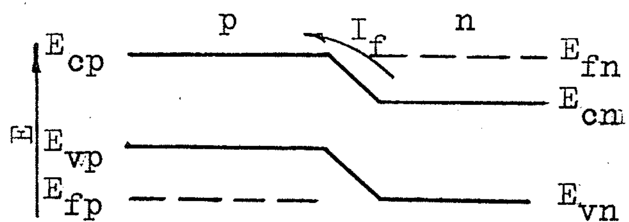

Fig. 2(d) HIGH FORWARD BIAS

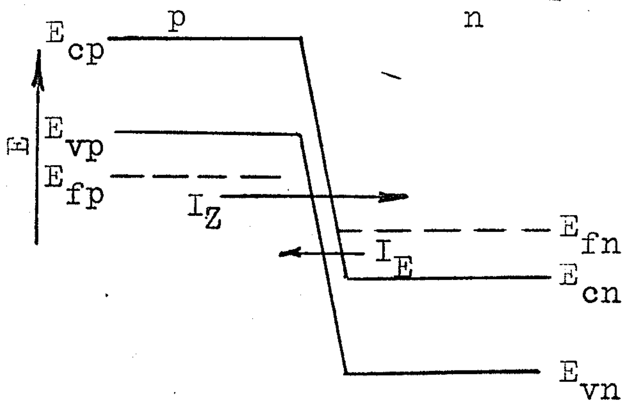

Fig. 2(e) REVERSE BIAS

If band tailing is assumed negligible $\rho_c(E)$ and $\rho_v(E)$ are given by:

$$\rho_c(E) = B(E - E_{cn})^{\frac{1}{2}} \quad \text{.......} 2.4$$

$$\rho_v(E) = C(E_{vp} - E)^{\frac{1}{2}} \quad \text{.......} 2.5$$

where B and C are constants. The energy levels E_{cn} and E_{vp} are defined in Figure 2(a).

Actually the Fermi-Dirac probability was derived for the case of complete random distribution of electron velocities and hence only applies at zero external bias. If, however, the field is small, as it is in the body of the semiconductors, the Fermi-Dirac statistics can be considered approximately applicable for low external biases. At the abrupt junction region, the fields are very high and the statistics cannot be applied.

If a slight forward bias is applied to the junction, the n side of the energy band diagram is elevated and there are states in the n side whose probability of being occupied is less than $\frac{1}{2}$. The result is an increase in I_E and a decrease in I_Z. As the forward bias is increased, a point is reached where any further increase in bias will cause the occupied states in the n side to come opposite the band gap on the p side, making direct tunneling impossible. This is known as the condition of peak bias and is shown in Figure 2(b).

As the bias is increased past the peak point, a point is eventually reached where E_{cn} is equal to E_{vp} and no direct tunneling can take place. The only current flowing at this point should be the conventional diode drift minus diffusion current, which would be negligibly small. The energy band diagram for this bias condition is shown in Figure 2(c).

At voltages up to slightly exceeding the peak point I_E and I_Z are the only currents of appreciable value to flow. Hence for this range of biases the net diode current I_b is given by:

$$I_b = I_E - I_Z \qquad 2.6$$

If the tunneling probabilities Z_{cv} and Z_{vc} are assumed equal, a relationship between I_E and I_z can be obtained from equations 2.1 and 2.2 as given in 2.7:

$$I_E(1 - f_c)f_v = I_Z(1 - f_v)f_c \qquad 2.7$$

Using equation 2.3 and the fact that

$$E_{fn} = E_{fp} + eV \qquad 2.8$$

where V is the applied voltage, gives:

$$f_c(1 - f_v) = f_v(1 - f_c)\exp.(eV/kT) \qquad 2.9$$

Combining equations 2.9, 2.7, and 2.6 gives:

$$I_E = I_b(1 - \exp.(-eV/kT))^{-1} \quad \text{......................2.10}$$

$$I_Z = I_b(\exp.(ev/kT) - 1)^{-1} \quad \text{......................2.11}$$

Curves of I_E and I_Z versus bias voltage are given in Figure 3.

Excess Current

Experimentally the current in the valley region is found to be considerably greater than the sum of the two direct tunneling currents (I_E and I_Z), and the conventional diode current I_f. This additional current is termed the "excess current", I_x.

Considerable research has been done on the mechanism of I_x. It has been discovered experimentally[9] that the excess current exhibits much the same dependence on pressure, temperature and doping concentrations as the tunneling currents do. From this it is assumed that some kind of a tunneling process must be involved. Since direct tunneling is impossible at the biases considered, an indirect tunneling process by way of localized energy states in the band gap is considered to be the mechanism of I_x. This theory has been confirmed[10] by deliberately changing the imperfection content of the crystal by radiation damage or doping. A theory that electrons could tunnel directly, losing energy in the process through photon emission, has not been proven and is generally discounted[8,9].

Figure 2(d) shows the condition producing the excess current. The main sources of the band gap states are:

1. Band edge tailing in degenerate semiconductors.

2. Donor or acceptor chemical impurities which become clustered due to high doping levels.

3. Unwanted chemical elements present.

4. Crystal defects such as slipped planes, missing atoms, or dislocated atoms.

The basic indirect tunneling path is thought to be that given by a b c in Figure 2(d). The electrons from the conduction band fall into an available state in the band gap (b), from which they tunnel into an unoccupied state in the valence band. On the basis of this mechanism, the following expression for the excess current is given[8]:

$$I_x = AN_xP_x \qquad \text{2.12}$$

where A is a constant, N_x is the density of occupied band gap states above the top of the n side valence band and P_x is the pertinent tunneling probability.

The approximate I_x for a G.E. 1N2939 diode is shown in Figure 3.

Conventional Diode Forward Current

If the bias voltage is increased beyond the valley point, the potential barrier is reduced sufficiently so that the

diffusion current of a conventional diode becomes appreciable and takes over. The net forward current I_f is equal to the diffusion minus drift current and is given by:

$$I_f = I_s(\exp.\ eV/kT - 1) \qquad 2.13$$

where I_s is the drift current. The approximate I_f for a 1N2939 tunnel diode is shown in Figure 3.

Reverse Current

If the diode is reverse biased, the energy band diagram is as shown in Figure 2(e). The filled states in the p side are now opposite empty states in the n side and the Zener current increases without bound until the junction overheats and burns out. This gives the diode a high dynamic conductance in the reverse bias region.

Figure 3 TUNNEL DIODE JUNCTION CURRENTS

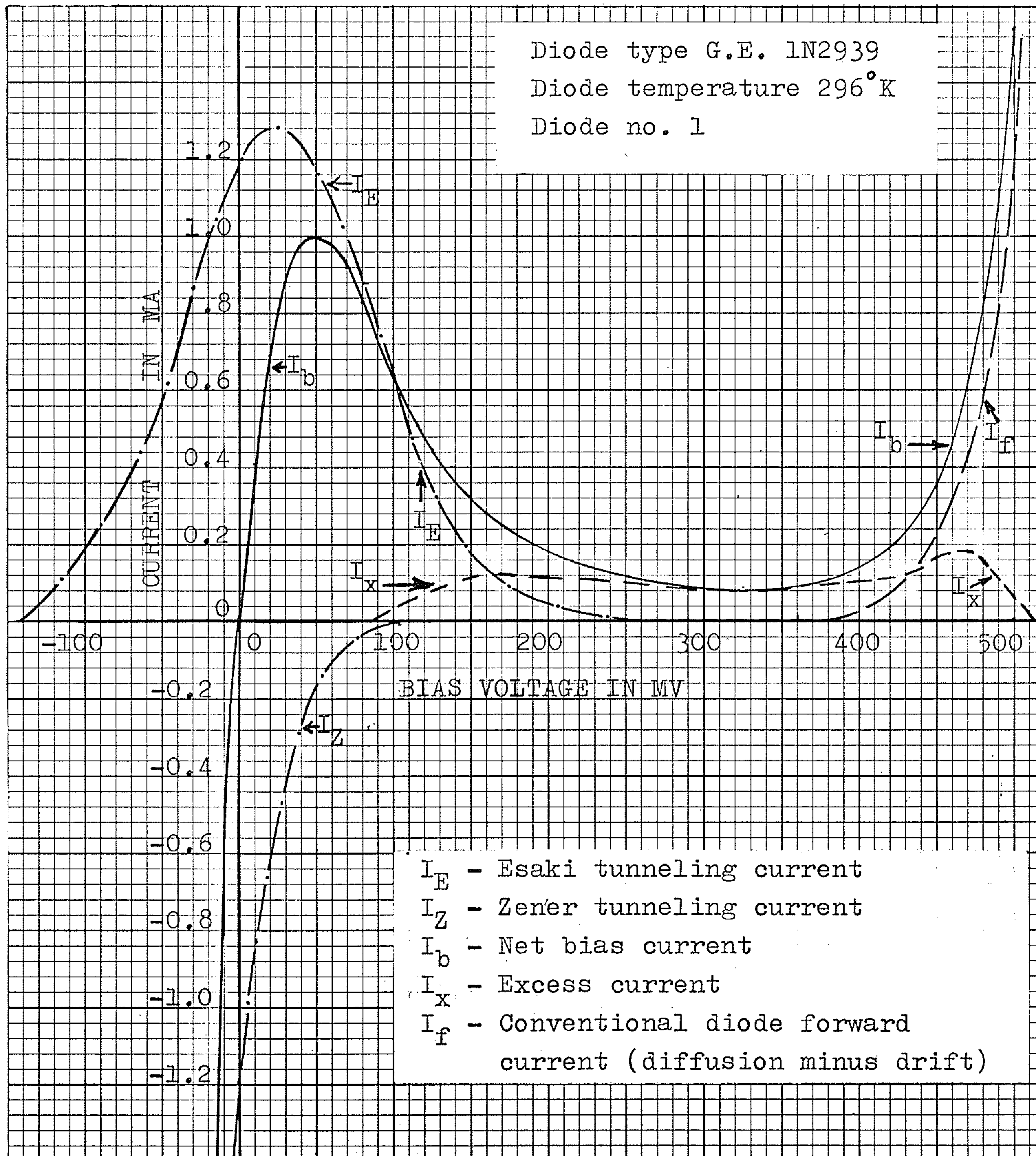

CHAPTER III

NOISE IN ELECTRONIC COMPONENTS

Electrical noise is defined as any spurious or undesired disturbance which tends to obscure a desired signal. The amount of noise produced in any electronic component sets a fundamental limit on its usefulness in any communications circuit.

Electrical noise can be divided into two broad catagories, 1) noise of an eliminable character and 2) fluctuation noise. The former is also called man-made and includes noise due to poor contacts, equipment vibration, ignition radiation, etc. By proper shielding, relocation of equipment or use of filtering circuits, this type of noise can be completely eliminated or at least minimized. The second type of noise is due to spontaneous fluctuations which occur throughout all physical quantities due to their noncontinuous, granular atomic nature.

Fluctuation noise produced in resistors, vacuum tubes, and semiconductors will be discussed in this chapter.

I NOISE IN RESISTORS

Two types of fluctuation noise are produced in resistors. They are called thermal and contact noise.

Thermal Noise

All conductors contain a large number of free electrons

and bound ions. At any temperature above absolute zero, the electrons have freedom of movement while the ions vibrate about their average position. Collisions between the electron and ions impart a completely random motion to the electrons. This gives rise to a random fluctuating current. Over a long period of time the net current will be zero. Instantaneous amplitude of this current will have a Gaussian distribution about zero. The current variations give rise to minute voltage fluctuations which can be detected by sensitive measuring circuits. This type of noise is called "thermal noise" because of its temperature dependence.

Thermal noise was first studied experimentally by Johnson[11] in 1927. His work was confirmed theoretically by H. Nyquist[12]. They showed that the mean square thermal noise voltage $\bar{v}^2_{nt}$ generated by an impedance Z is given by:

$$\bar{v}^2_{nt} = 4kTRB \qquad (3.1)$$

where k is Boltzmann's constant, T is the impedance temperature in degrees Kelvin, R is the resistive component of Z in ohms, and B is the noise bandwidth of the measuring device.

Thermal noise present in a resistor R can be represented by either a voltage generator in series with R, or by a current generator in shunt with R as shown in Figure 4.

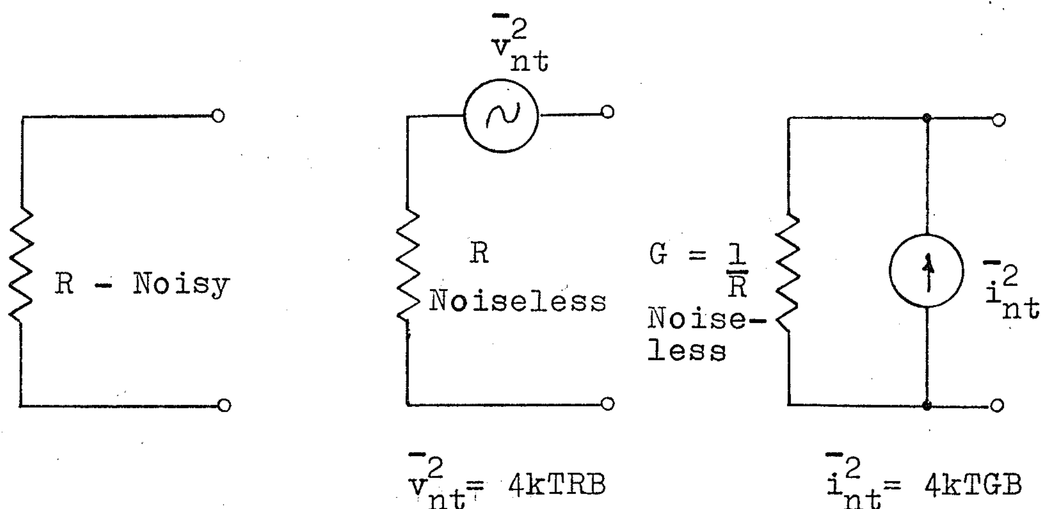

Figure 4 REPRESENTATION OF RESISTOR THERMAL NOISE

The noise voltages or currents from different resistors are considered uncorrelated and must be added as mean square quantities. The thermal noise produced by a passive network can be found by finding the equivalent impedance of the network and then applying equation 3.1. Another method would be to apply equation 3.1 to each impedance and then combine the resulting current or voltage generators.

Thermal noise has a constant spectrum up to very high frequencies, and so it is termed "white noise". Actually its spectrum cannot be constant for all frequencies or the available noise power would be infinite. At higher frequencies the kT in equation 3.1 is replaced by kT/(exp.hf/kT - 1), where h

is Planck's constant (6.63×10^{-34} joule-seconds) and f is the frequency considered. At room temperature the correction is negligible below 1000 megacycles.

Noise Bandwidth

The noise bandwidth of a device with transfer function $H_{(j\omega)}$ is defined as the width of an ideal bandpass filter transfer function which has an absolute value of the maximum value of $H_{(j\omega)}$, and delivers the same power from a white noise source. Stated mathematically the definition is given by:

$$B = \frac{1}{A_m^2} \int_0^{\infty} \left| H_{(j\omega)} \right|^2 df \quad \ldots\ldots 3.2$$

where A_m is defined in Figure 5.

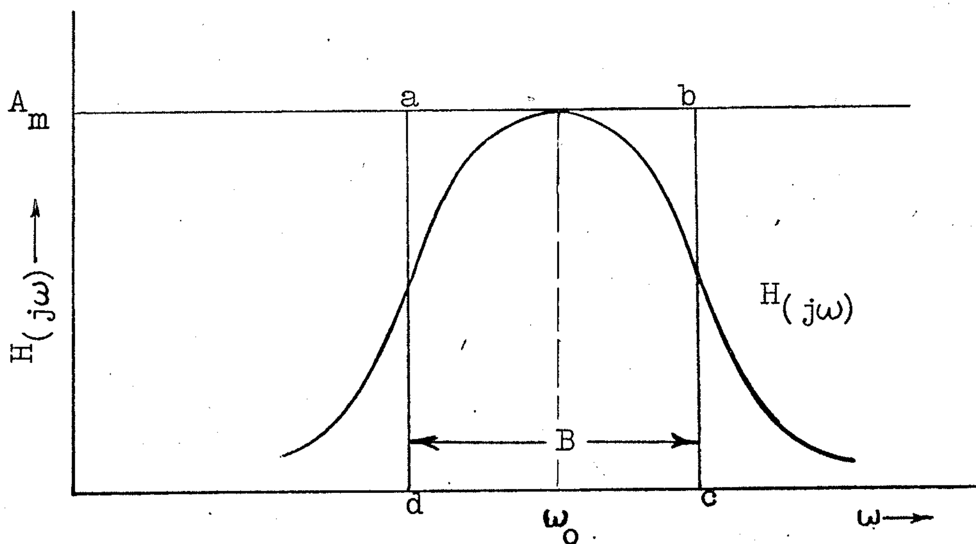

FIGURE 5 EQUIVALENT NOISE BANDWIDTH

Contact Noise

Carbon composition resistors consist of a large number of very small conducting particles in more or less loose contact. This causes minute changes in resistance which produce noise in the resistor in excess of thermal noise. This excess noise is called contact noise. It has been investigated by Christenson and Pearson[13], and was found to exhibit a 1/f spectrum. Contact noise is negligible at 1 megacycle in comparison to thermal noise.

II NOISE IN VACUUM DIODES

The two important types of fluctuation noise in vacuum tubes are shot noise and flicker noise.

Shot Noise

Shot noise is commonly defined as the spontaneous fluctuations in the plate current of a vacuum diode due to the random emission of discrete electric charges (electrons) from a hot cathode. The name shot noise is derived from the resemblance of this electron frow to a stream of shot. Shot noise is not confined to vacuum tubes but occurs wherever this combination of discreteness and random emission are found.

Shot noise in vacuum diodes was first investigated by Schottky. He derived the formula for the mean square shot noise current of a temperature limited vacuum diode as:

$$\overline{i^2_{ns}} = 2eIB \qquad (3.3)$$

where I is the average plate current and B the noise bandwidth of the measuring device.

At frequencies approaching the electron transit time there is a reduction in the shot noise of a vacuum diode. The accurate formula for high frequencies is given by van der Ziel[14a], as:

$$\overline{i^2_{ns}} = \frac{2eIB}{1 - \omega^2\tau^2/18} \qquad (3.4)$$

where ω is the angular frequency, and τ the transit time in seconds. The correction is negligible below 100 megacycles for most diodes.

If a vacuum diode is operated in its temperature limited region its impedance is infinite and the shot noise produced may be represented by an ideal current generator. The equivalent noise circuit of such a diode is given in Figure 6.

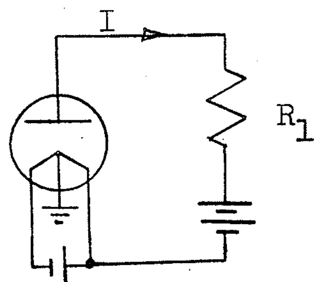

Temperature limited vacuum diode

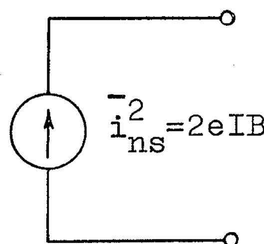

Equivalent shot noise current generator

Figure 6 REPRESENTATION OF VACUUM DIODE SHOT NOISE

Flicker Noise

At low frequencies the noise produced by vacuum diodes is considerably more than that given by equation 3.3. This excess noise is termed "flicker noise". Like the excess contact noise in resistors, it also has a 1/f spectrum. At frequencies above about 10 kilocycles it becomes negligible compared to the shot noise[15a].

The exact mechanism producing flicker noise is still not completely understood. It is thought that changes in emission from relatively large areas of the cathode and resistance between the cathode base metal and oxide coating are responsible.

Use of Temperature Limited Vacuum Diode as a Noise Generator

From the preceding discussion it is obvious that a vacuum diode could be used as a calibrated noise source. In order that equation 3.3 applies, the following precautions must be taken:

1. The diode noise should not be used below 10 kilocycles or above 100 megacycles.

2. The diode must be operated in its temperature limited region.

3. The plate and filament supplies should be filtered to prevent any external signal from entering into the circuit.

4. A variable filament supply must be used to vary the plate current and hence the noise output.

A Sylvania type 5722 noise diode was used as a noise source for all noise measurements performed. This diode is constructed so that transit time effects are negligible below 500 megacycles.

The complete circuit for the 30 megacycle noise generator is given in Figure 7.

The combination of chokes and capacitators in the plate and filament supply circuits prevented any stray 30 megacylce signal from entering via those sources.

The Lambda regulated power supply used as a filament supply gave a continuously variable output of 0 to 5 amperes at 0 to 30 volts.

The 1000 ohm load resistor gave temperature limited operation with 150 volts on the plate.

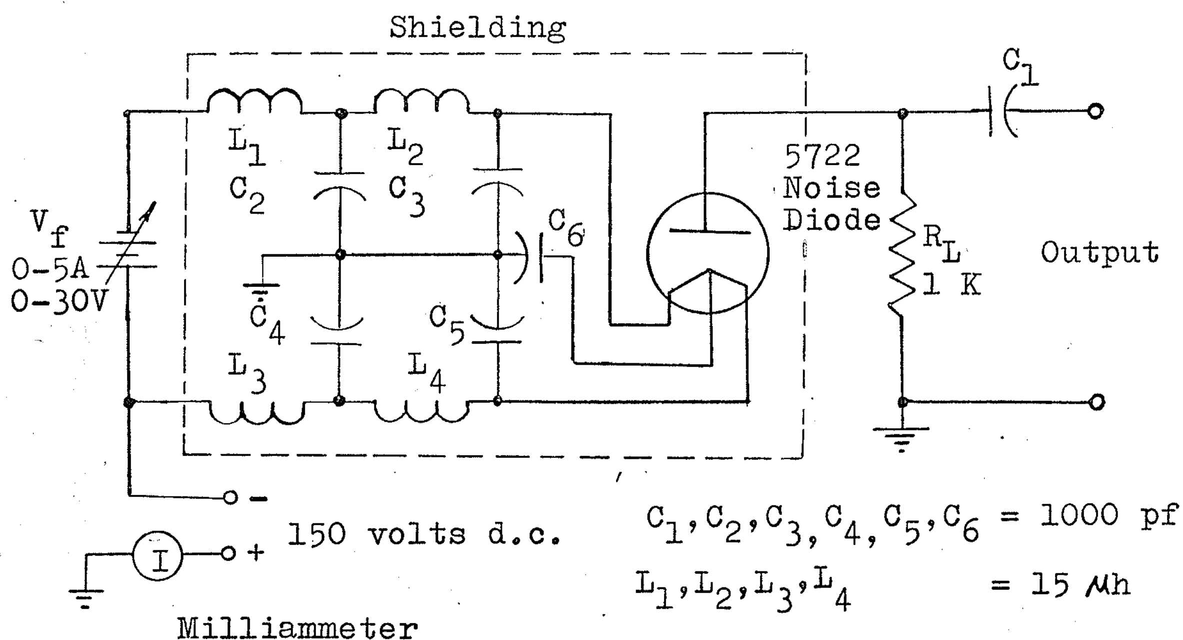

Figure 7 CIRCUIT DIAGRAM OF NOISE GENERATOR

The meter used to read the plate current had ranges from 0.1 to 10 milliamperes.

Two factors which could reduce the noise power output of a diode are its output capacitance Co and lead inductance L. The correction due to these factors to $\overline{i^2_{ns}}$ is $(\omega^2 LCo - 1)^{-2}$. For a 5722 (Co $\cong$ 2pf, L $\cong$ 10 nh) the correction is negligible at 30 megacycles.

III NOISE IN SEMICONDUCTORS

The spreading and contact resistance (R_s) of a semiconductor device exhibits thermal noise. The mean square noise voltage generated is given by:

$$\overline{v^2_{nt}} = 4kTR_sB \qquad 3.4$$

Since the current across a p-n junction consists of the superposition of a large number of independent, random events involving discrete current carriers, the junction currents exhibit full shot noise[15b]. The mean square noise current generated is given by:

$$\overline{i^2_{st}} = 2eI_jB \qquad 3.5$$

where I_j is the junction current under consideration.

Semiconductors also exhibit noise similar to flicker

noise in vacuum tubes. This noise is commonly called "excess" or "1/f" noise. The spectral density of this noise is inversely proportional to frequency. Van der Ziel[14b] gives the following formula for the mean square excess noise current:

$$\overline{i}^2_{ex} = KI_j^a B f^{-b} \qquad 3.6$$

where K is a constant, I_j is the junction current and f is the frequency. The constants a and b are close to 2 and 1 respectively. Experiments performed by Mattson and van der Ziel[16] indicate excess noise is found up to about 10 megacycles.

CHAPTER IV

THEORETICAL TUNNEL DIODE NOISE MODEL

In this chapter a discussion of noise in the theoretical model of a tunnel diode will be given. The noise contributed by the various junction currents outlined in Chapter II will be calculated. The diode's equivalent noise resistance will be discussed.

Simplified Equivalent Circuit

As a first approximation to the equivalent circuit of a tunnel diode, consider simply a resistance equal in value to the diodes dynamic resistance R_d. The value of R_d is found by taking the slope of the diode's V-I curve at any bias . From Figure 1 it can be seen that for a 1N2939 diode at zero bias, R_d is about 20 ohms, and at peak bias (V_p) it is infinite. In the region between peak bias and valley bias (V_v), R_d is negative and has a minimum absolute value of about 100 ohms. At biases above V_v, R_d decreases rapidly and approaches zero.

If a bias voltage V is applied to R_d, a current I_b flows. Since each of the currents composing I_b is due to a different mechanism, they are considered uncorrelated. If it is assumed they all produce full shot noise, the total mean square shot noise current produced would be given by:

$$\overline{i^2_{ns}} = 2e(I_E + |I_Z| + I_x + I_f)B \quad \text{......................} \quad 4.1$$

The theoretical equivalent shot noise current (I_n) of a tunnel diode is defined by:

$$\overline{i}^2_{ns} = 2eI_nB \quad \text{.....} 4.2$$

From equations 4.1 and 4.2 we have:

$$I_n = I_E + |I_Z| + I_x + I_f \quad \text{.....} 4.3$$

<u>Noise due to Tunneling Currents</u>

If biases only to a point slightly exceeding the peak point are considered, I_b is composed of only the two tunneling currents as shown in Figure 3. For this range of biases :

$$I_b = I_E - |I_Z| \quad \text{.....} 4.4$$

and

$$I_n = I_E + |I_Z| \quad \text{.....} 4.5$$

Combining equations 2.10 and 2.11 with 4.4 and 4.5 gives:

$$I_n = I_b \operatorname{Coth} eV/2kT \quad \text{.....} 4.6$$

In equation 4.6 for a given I_b, V is the voltage across the junction. It differs from the external bias voltage by the voltage drop in the spreading resistance R_s. Equation 4.6 is valid only for the region up to slightly exceeding the peak point. For the remainder of the characteristic

I_n will be equal to I_b . A plot of I_n versus bias voltage for one of the diodes tested is given in Figure 8.

Excess Noise in the Valley Region

In the previous discussion it was assumed that all currents exhibit only full shot noise. Noise measurements performed on tunnel diodes so far[4,5,6] all indicate that I_x produces considerably more than shot noise.

Tiemann[4] proposes that there could be deep level states present in the band gap due to some unknown impurity or a complex of donor and acceptor atoms. If the bound states have a lifetime of greater than $2x10^{-19}$ seconds, the noise produced could exceed shot noise by a measurable amount.

Agourdis and van der Vliet[5] propose that I_x cannot be attributed to random events. They don't consider it likely I_x is composed of two opposite tunneling currents.

Noise at Higher Forward Biases

At high forward biases (500 mv for the 1N2939) the tunnel diode acts like a conventional diode. The junction currents that flow are a reverse drift current I_s and a forward diffusion current I_s exp. eV/kT. Each is considered to exhibit full shot noise[16] and so at large forward biases I_n is given by:

$$I_n = I_s \exp. eV/kT + I_s \quad \text{..............................4.7}$$

The net forward current I_f is given by:

$$I_f = I_s \exp. eV/kT - I_s \quad \ldots\ldots 4.8$$

Combining 4.7 and 4.8 gives:

$$I_n = I_f + 2I_s \quad \ldots\ldots 4.9$$

At the biases considered, $2I_s$ is negligible compared to I_f .

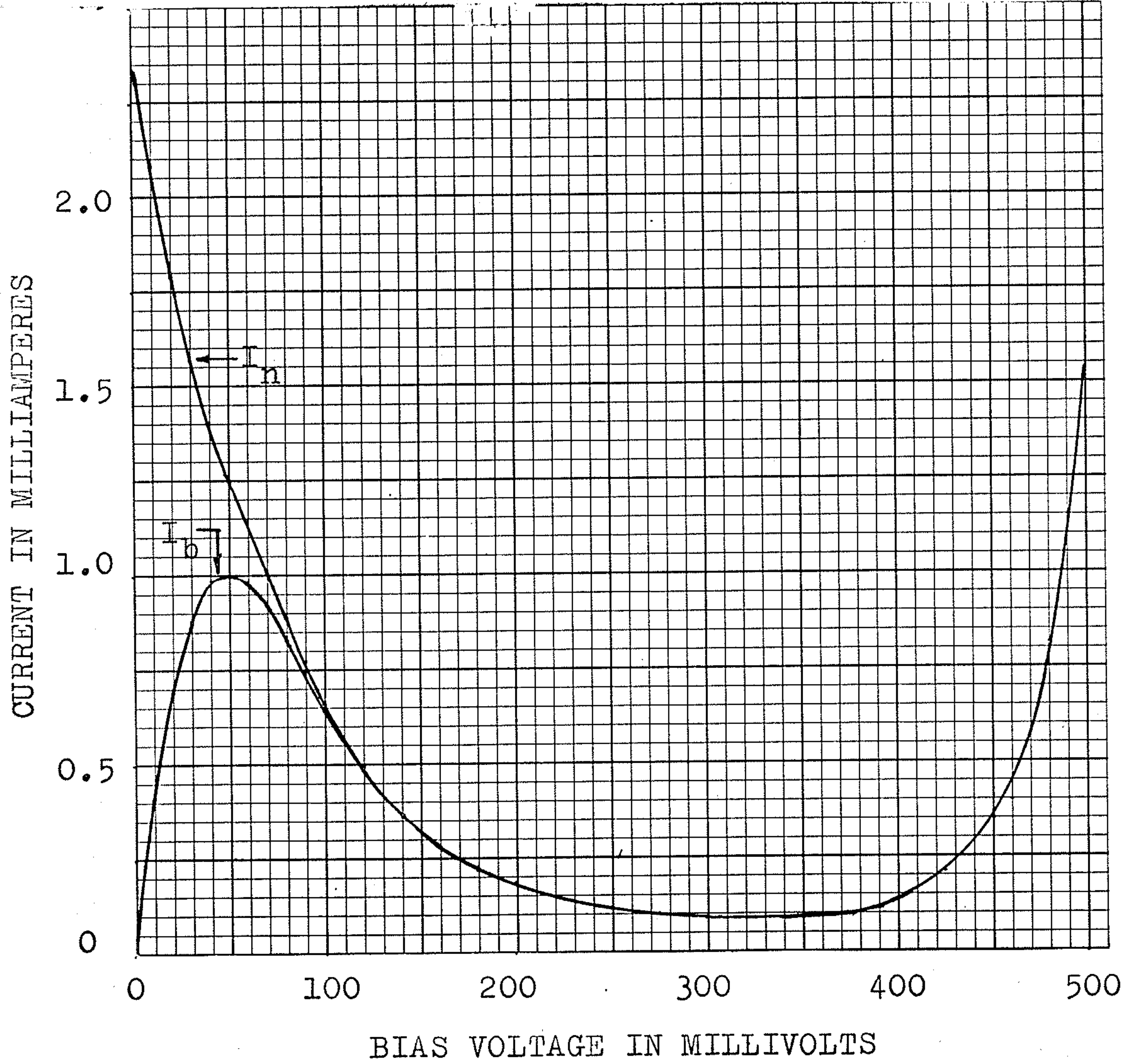

Figure 8 TUNNEL DIODE THEORETICAL EQUIVALENT NOISE CURRENT

From the preceding discussion it is obvious that to be able to calculate I_n an accurate V-I characteristic must be obtained. Appendix A.1 gives the method used to obtain such a characteristic of the diodes tested.

Equivalent Noise Resistance

The amount of noise produced by a diode can also be compared with the noise produced by an equivalent noise Resistance (R_n). R_n is defined as a resistance exhibiting only thermal noise which produces a mean square noise voltage equal to that produced by a tunnel diode. The definition is illustrated in Figure 9.

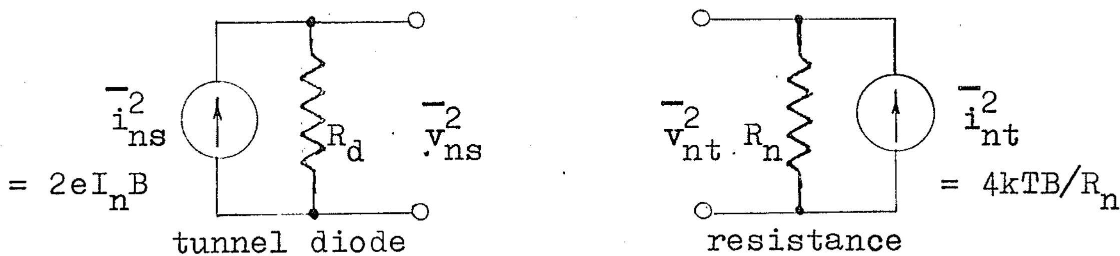

Figure 9 TUNNEL DIODE EQUIVALENT NOISE RESISTANCE

If $\overline{v^2_{ns}} = \overline{v^2_{nt}}$ then the diode noise resistance is given by:

$$R_n = eI_nR_d^2/2kT \quad \text{.........} \quad 4.10$$

A plot of the noise ratio R_d/R_n is given in Figure 10.

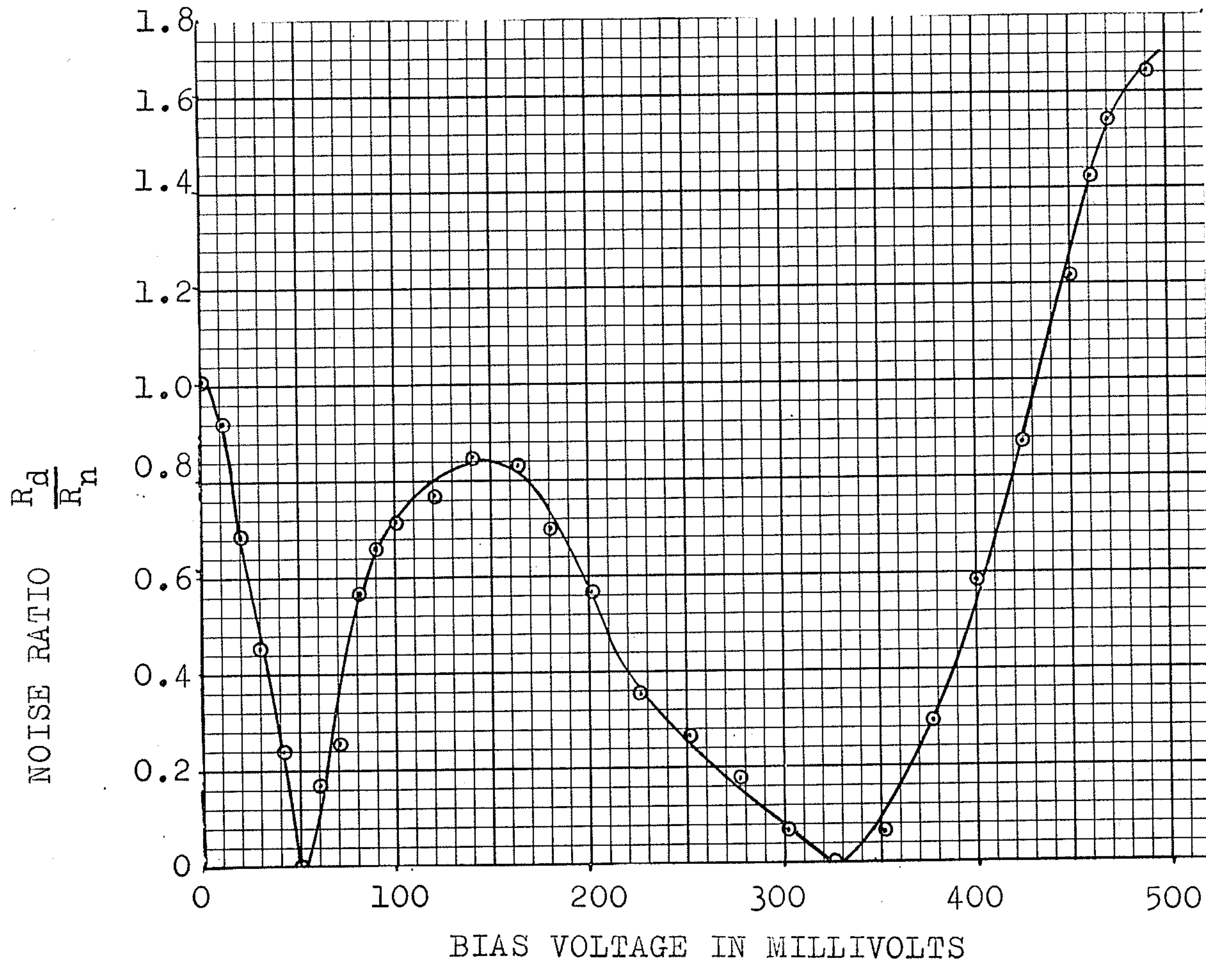

Figure 10 RATIO OF TUNNEL DIODE DYNAMIC TO NOISE RESISTANCE

The plot of Figure 10 shows that the tunnel diode noise resistance is greater than its dynamic resistance for almost the whole range of its characteristic. At zero bias the ratio R_n/R_d is equal to one, since at this point the diode is in a state of thermal equilibrium and can be considered to exhibit thermal noise. This can be proven by rewriting equation 4.6 as:

$$I_b = I_n \mathrm{Tanh}(eV/2kT) \qquad \ldots 4.11$$

Now R_d is given by:

$$R_d = \frac{dV}{dI_b} = \frac{2kT}{eI_n} \mathrm{Cosh}(eV/2kT) \qquad \ldots 4.12$$

At zero bias equation 4.12 reduces to:

$$R_d \Big|_{V=0} = 2kT/eI_n \qquad \ldots 4.13$$

Substituting this value for R_d in equation 4.10 gives:

$$R_d/R_n \Big|_{V=0} = 1 \qquad \ldots 4.14$$

At high forward biases the tunnel diode acts as a conventional diode. At these biases the dynamic resistance of a conventional diode is given by:

$$R_d \Big|_{V>V_v} = kT/eI_b \qquad \ldots 4.15$$

From the discussion in Chapter III, I_n is given by I_b at these biases. Using this fact and equation 4.15, equation 4.10 becomes:

$$R_d/R_n \Big|_{V>V_v} = 2 \qquad \ldots 4.16$$

From Figure 10 it is seen that at a forward bias of 500 millivolts the ratio R_d/R_n approaches 2.

CHAPTER V

EFFECT OF PARASITIC ELEMENTS ON I_n

The equivalent circuit of Chapter IV does not hold for a physical tunnel diode. Parasitic elements, such as lead inductance, semiconductor bulk resistance, and junction capacitance, which exist in a physical diode will have an effect on the theoretical noise produced by the junction currents. This effect will be discussed in this chapter.

Exact Equivalent Circuit

The accepted small signal equivalent circuit of a tunnel diode[19] is given in Figure 11 below.

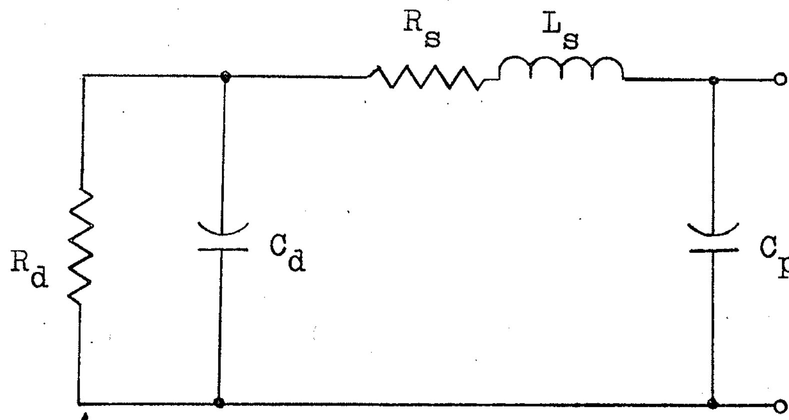

Figure 11 TUNNEL DIODE EQUIVALENT CIRCUIT

R_d is the diode's dynamic resistance. It can be positive or negative depending on the bias voltage.

C_d is the junction capacitance. It varies with the bias voltage V according to the equation $C_d=(\phi-V)^{-\frac{1}{2}}$, where K

is a constant and ϕ the built-in potential of the junction.

R_s is the series spreading and contact resistance. It is independent of bias voltage.

L_s is the lead and package inductance. It varies greatly with lead length.

C_p accounts for the package and lead capacitance. It is less than 1 pf for modern packages and will be neglected.

The techniques used to measure the various circuit elements are given in Appendix A. The results are tabulated in Table I below.

Table I TUNNEL DIODE EQUIVALENT CIRCUIT ELEMENT VALUES

Tunnel diode no.	1	2	3	G.E. specs.
$\lvert -R_d \rvert_{min.}$ in ohms	98	114	95	150
C_d at V_p in pf	7	6.5	7.5	5
C_d at V_v in pf	9	8	10	
R_s in ohms	2.5	2.3	2.0	1.5
L_s in nh	43**	39**	35**	6*

* For 1/8 inch leads

**For 3/8 inch leads

Equivalent Noise Circuit

The equivalent noise circuit for a tunnel diode is now as shown in Figure 12 below.

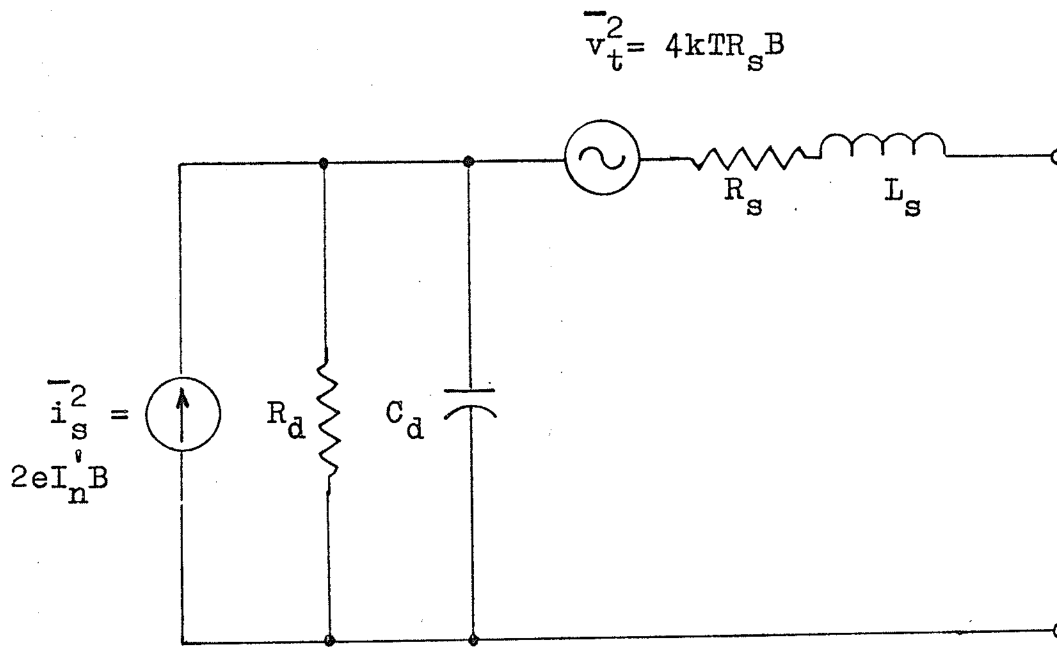

Figure 12 TUNNEL DIODE EQUIVALENT NOISE CIRCUIT

By changing the shot noise current generator to a voltage generator, combining it with the thermal noise voltage generator and then changing back to a single current generator, the following noise circuit is obtained.

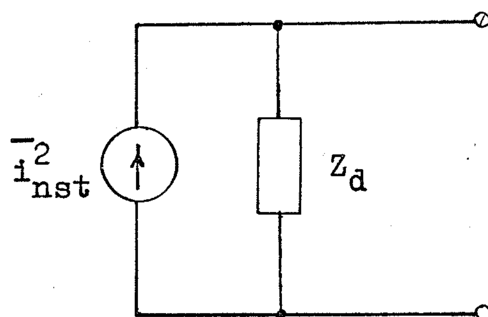

Figure 13 TUNNEL DIODE SHUNT EQUIVALENT NOISE CIRCUIT

The current generator in Figure 13 is given by:

$$\overline{i}^2_{nst} = \frac{4kTR_sB + 2eI_nR_d^2B(1+\omega^2R_d^2C_d^2)^{-1}}{(R_s+R_d(1+\omega^2R_d^2C_d^2)^{-1})^2 + (\omega L_s-\omega R_d^2C_d^2(1+\omega^2R_d^2C_d^2)^{-1})^2} \quad \ldots\ldots 5.1$$

A corrected theoretical equivalent shot noise current I_n' is defined by:

$$I_n' = \overline{i}^2_{nst}/2eB \quad \ldots\ldots 5.2$$

Values of I_n' as calculated using an I.B.M. 1620 computer are shown in Figure 14. The parasitic elements were found to have a negligible effect on I_n in the negative resistance region, and for that reason only the two positive conductance regions are shown in Figure 14.

A problem exists in calculating I_n at very low forward biases as the varible Coth eV/2kT in equation 4.6 goes to infinity as V goes to zero. To get around this problem a very accurate digital voltmeter (0.1%) was used to measure both the diode current and voltage. The measured voltage was corrected for the drop across R_s giving an accurate value for V. Also at zero bias I_n can be replaced by the equivalent noise current of R_d which can be measured accurately on a bridge as given in Appendix A. The measured diode resistance was corrected for R_s to give the true value of R_d.

By varying the values of the different elements in

Figure 14 EFFECT OF PARASITIC ELEMENTS ON I_n

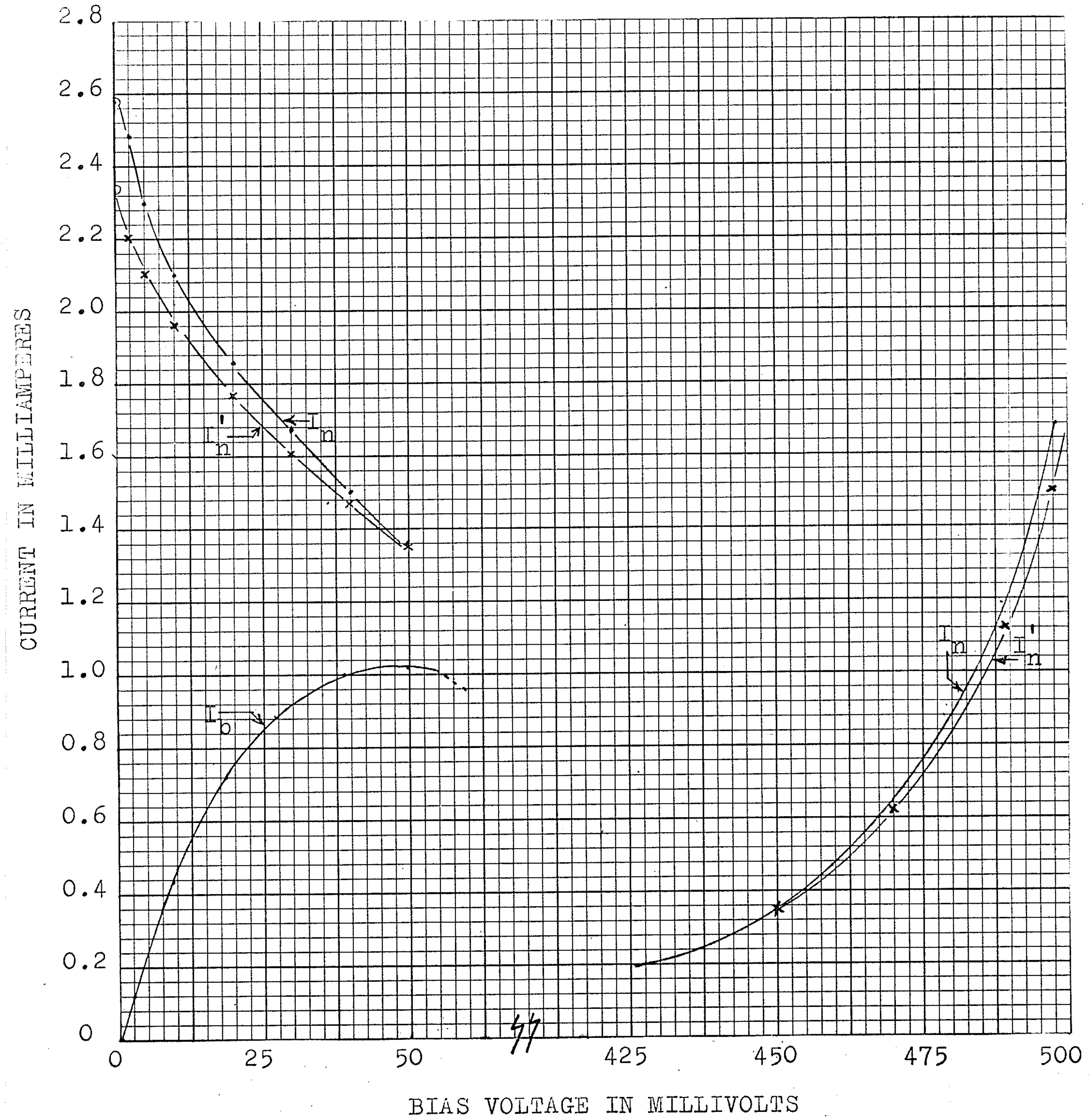

equation 4.3 it was evident that the largest effect on I_n is due to R_s. This is as expected since at zero bias R_s is about 10% of R_d.

CHAPTER VI

NOISE MEASUREMENTS

In performing noise measurements on any electronic component, the general method used is to compare its noise output with that produced by a calibrated source. To make this comparison, a high gain linear amplifier and a square law detector are usually used. If a substitution method is used, the input impedance to the amplifier is kept constant and the detector need not be square law to detect two equal power levels. Two variations of the substitution method were used and are outlined in this chapter.

I WIENS METHOD

The first method of making noise measurements was developed by Wiens[2]. The test circuit used is given in Figure 15. The exact circuit for the noise generator is given in Figure 7.

The component under test was connected to the noise generator with the shortest practical leads to minimize inductance and pickup.

A frequency of 30 megacycles was chosen because excess noise in vacuum diodes, resistors and semiconductors is negligible at this frequency.

The procedure followed is outlined below.

1. A resistor (R_1) is soldered on at terminals marked x - x .

With the noise diode filament voltage turned off, a signal of one millivolt is applied from the signal generator. This signal is large enough to swamp out the noise and yet not big enough to produce serious non linear effects when the resistor is replaced by the tunnel diode. The preamp gain is turned full up and the precision receiver gain adjusted until a convenient output reading I_1 is obtained.

2. The resistor R_1 is then replaced by the tunnel diode and stabilizing resistor R_2 combination. The stabilizing resistor must obey the stability criterion as given in Appendix A. A value of R_2 of about 70 ohms stabilizes the type 1N2939 tunnel diode everywhere in its negative conductance region. If the mesurement is performed in the two positive conductance regions, R_2 is omitted. With the same signal level and receiver gain as in 1., the tunnel diode bias is adjusted until the output meter again reads I_1. The following equality now holds:

$$G_2 - G_d = G_1 \qquad \text{6.1}$$

where G_d is the diode negative conductance, $G_1 = 1/R_1$ and $G_2 = 1/R_2$.

3. With all connections as in 2. the calibration signal is removed and the receiver gain increased until a convenient output reading I_2 is obtained. This reading is due to the following noise sources: i) the noise from the tunnel diode

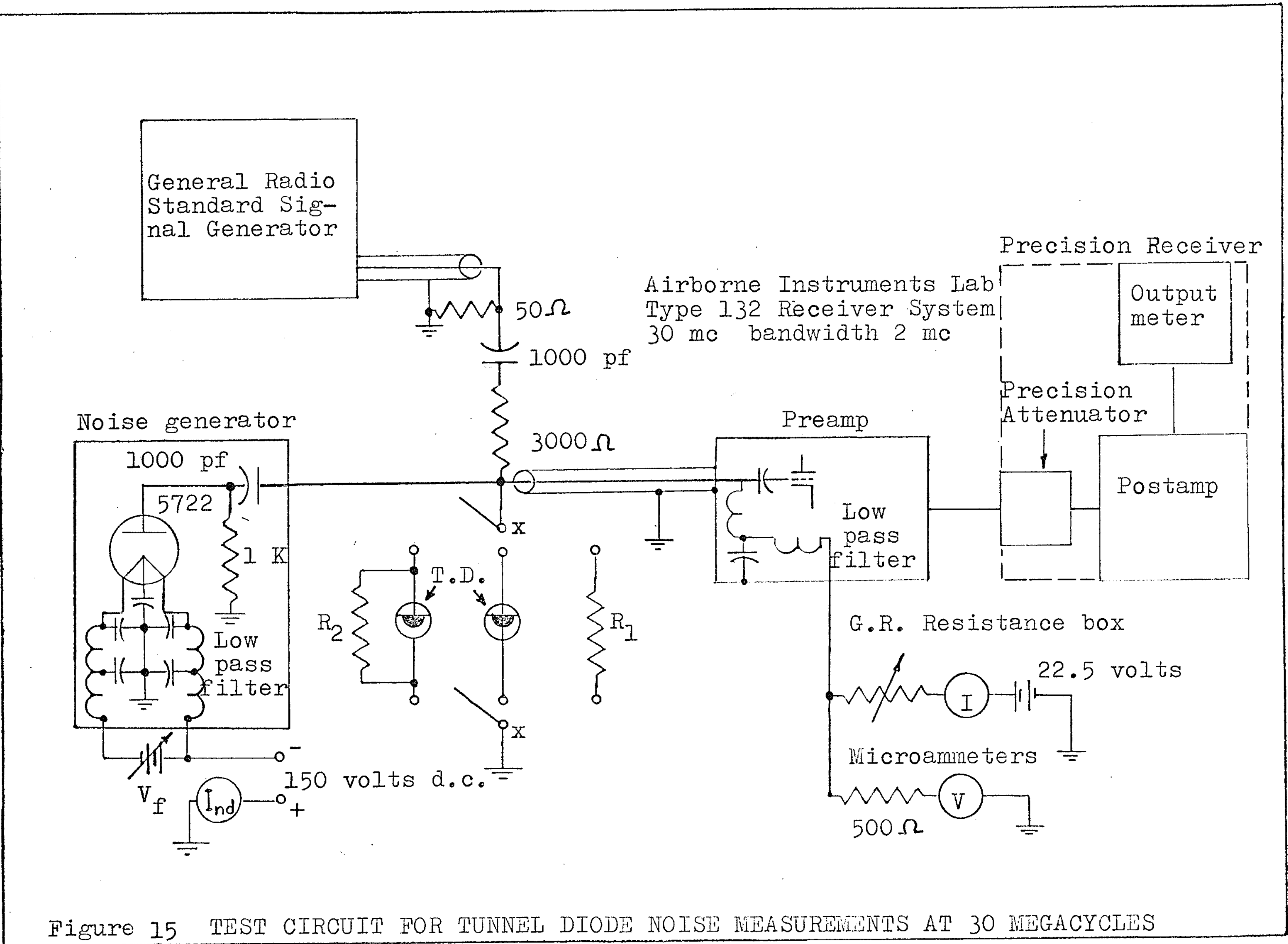

Figure 15 TEST CIRCUIT FOR TUNNEL DIODE NOISE MEASUREMENTS AT 30 MEGACYCLES

and its stabilizing resistor, ii) the noise from the preamp, the tunnel diode biasing resistor, the noise diode load resistor and all other resistances in the input circuit.

4. With all gain settings unchanged, the resistor R_1 is again placed in x - x. Noise is then added from the noise generator until an output reading of I_2 is again obtained. The noise diode plate current required I_{nd} is recorded. The output reading is due to noise from the following sources: i) the resistor R_1, ii) the noise diode, and iii) from the preamp, the tunnel diode biasing resistor, the noise diode load resistor and all other resistances in the circuit. Because the input impedance and gain are the same as in 3. the noise contribution from these sources will be the same as before.

Since all conditions in 3. and 4. are the same, the mean square noise currents from the different sources can be equated as follows:

$$2eI_{eq}B + 4kTG_2B = 2eI_{nd}B + 4kTG_1B \qquad 6.2$$

where I_{eq} is the tunnel diode experimental equivalent shot noise current. Rearranging equation 6.2 gives:

$$I_{eq} = I_{nd} + \frac{2kTG_1}{e} - \frac{2kTG_2}{e} \qquad 6.3$$

For measurements in the positive conductance region G_2 is zero

THE UNIVERSITY LIBRARY OF MANITOBA

and:

$$I_{eq} = I_{nd} + \frac{2kTG_1}{e} \qquad 6.4$$

The resistor conductances were measured to better than 1% on a Wayne Kerr V.H.F. admittance bridge. The temperature of all components was taken as being at room temperature since all components were sufficiently removed from any additional heat source.

The results obtained using this method are given in Figure 16.

II TEIMANN METHOD

The second method used to measure tunnel diode noise is a slight modification of that used by Tiemann[4]. The test circuit for this method is the same as for the previous method and is given in Figure 15. The only change is in the procedure which is given below:

1. A resistor R_1 of suitable value is placed in terminals x - x. With the signal and noise generators turned off, the preamp gain is turned full up and the receiver gain adjusted for a convenient reading I_1. The amplifier gain is then reduced by 3db using the precision attenuator. The output reading is then restored to I_1 by adding noise from the noise generator. The plate current of the noise diode required is care-

fully noted. The noise power from the noise diode equals that from the following sources: i) the resistor R_1, ii) the remaining preamp input circuit and the preamp itself.

I_{nd1} is thus the equivalent shot noise current of the resistor $R_1(I_{R_1})$ plus the amplifier and its input circuit(I_A). This gives:

$$I_{nd1} = I_{R_1} + I_A \quad \ldots\ldots\ldots\ldots\ldots\ldots\ldots\ldots\ldots\ldots\ldots 6.5$$

where $I_{R_1} = 2kTG_1/e$ and I_A depends on the preamp input termination and gain setting. Then with the noise diode turned off the output of the signal generator is increased until the output meter reads a convenient value, say I_2, compared to the noise level.

2. With the tunnel diode and its stabilizing resistor R_2 in the terminals marked, x - x, and the signal level and receiver gain unchanged, the diode bias is adjusted so that an output of I_2 is again obtained. The preamp input impedance and gain are now exactly as in 1. Under these conditions the preamp equivalent shot noise current will be as in 1. With the signal generator turned off, the receiver gain is adjusted for a convenient output reading, say I_3. The receiver gain is then decreased 3db and noise added from the noise diode until the output meter again reads I_3. The plate current of the noise diode I_{nd2} is recorded. Now I_{nd2} is the equivalent noise current of the tunnel diode (I_{eq}) plus the stabilizing resistor (I_{R_2})

plus the preamp and its input circuit (I_A). This gives :

$$I_{nd2} = I_{eq} + I_{R_2} + I_A \quad \text{.......... 6.6}$$

where $I_{R_2} = 2kTG_2/e$

Combining equations 6.6

$$I_{eq} = I_{nd2} - I_{nd1} - 2kT(G_2 - G_1)/e \quad \text{.......... 6.7}$$

For measurements in the positive conductance regions the stabilizing resistor is not required and:

$$I_{eq} = I_{nd2} - I_{nd1} + 2kTG_1/e \quad \text{.......... 6.8}$$

The results obtained by this method are shown for all three tunnel diodes tested in Figures 16, 17, and 18.

Comparison of Wiens and Tiemann Methods

The Wiens method has a basic disadvantage in that for a considerable range of biases the equivalent resistor R_1 produces more noise than the tunnel diode and its stabilizing resistor. Hence in order to use the method a negative I_{nd} must be extrapolated, which requires that the preamp be linear. The range of biases for which this occurs can be seen if equation 6.3 is rewritten using I_n instead of I_{eq}. This gives:

$$I_{nd} = I_n - (I_{R_1} - I_{R_2}) \quad \text{.......... 6.9}$$

Figure 16 COMPARISON OF EXPERIMENTAL AND THEORETICAL TUNNEL DIODE EQUIVALENT SHOT NOISE CURRENT

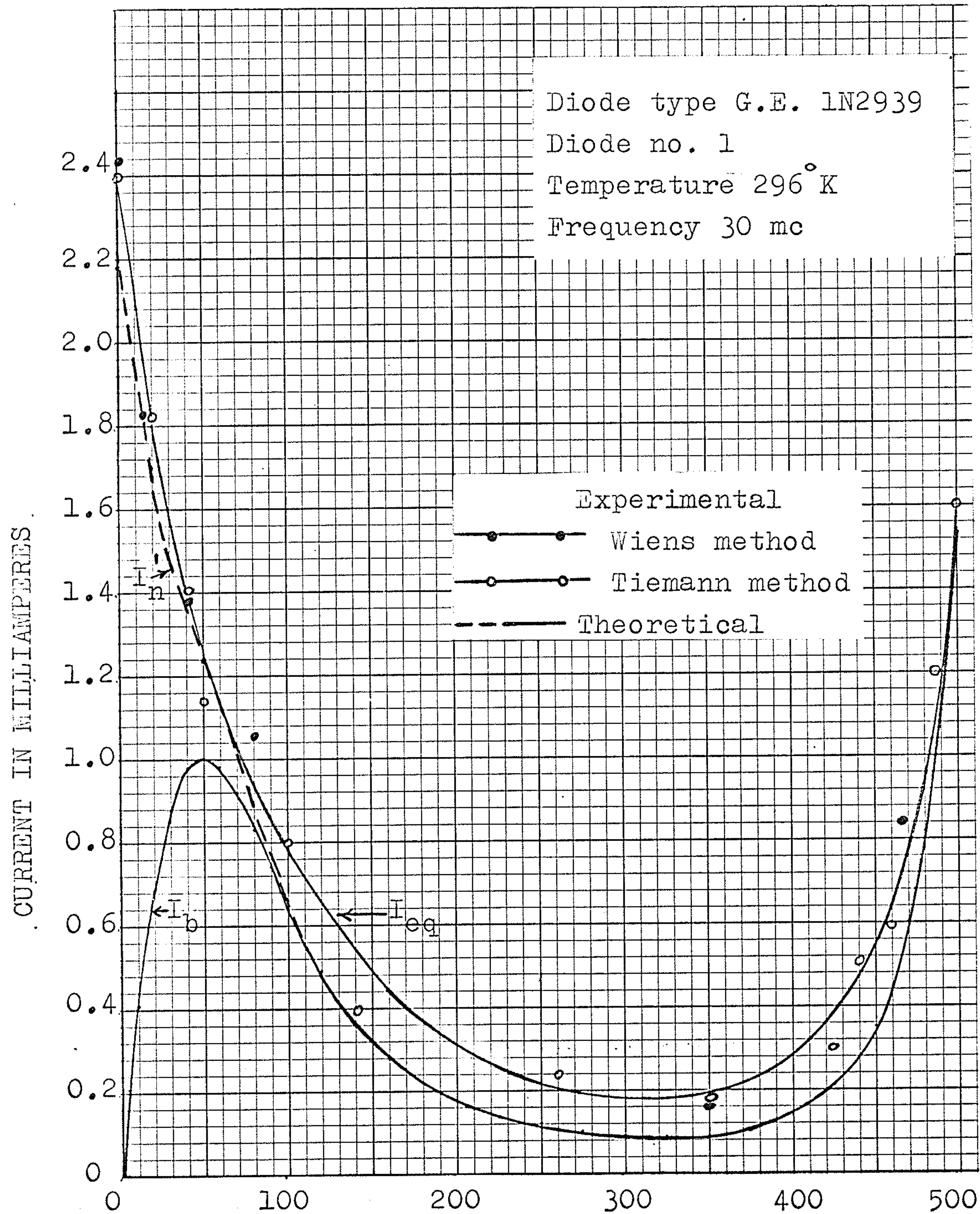

Figure 17 COMPARISON OF EXPERIMENTAL AND THEORETICAL TUNNEL DIODE EQUIVALENT SHOT NOISE CURRENT

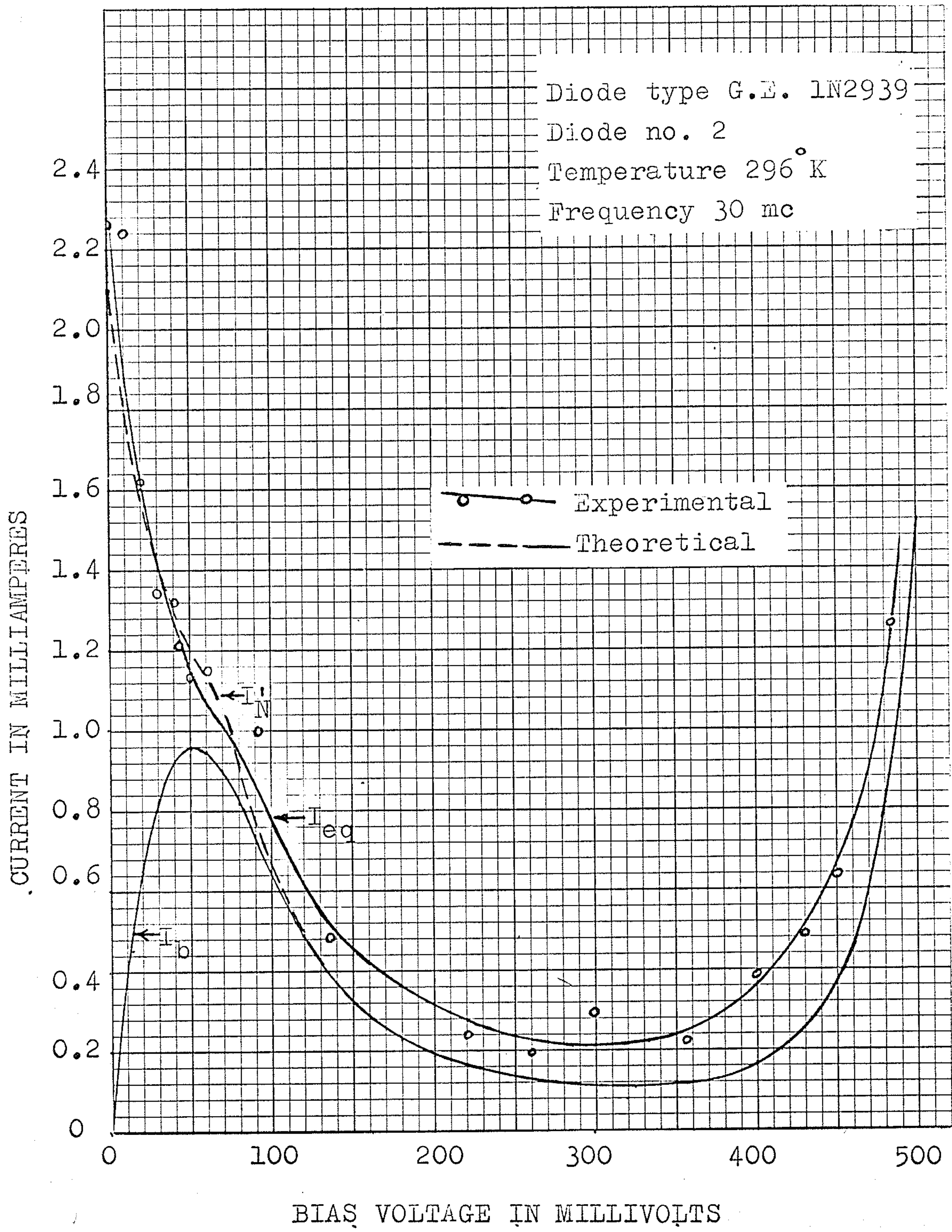

Figure 18 COMPARISON OF EXPERIMENTAL AND THEORETICAL TUNNEL DIODE EQUIVALENT SHOT NOISE CURRENT

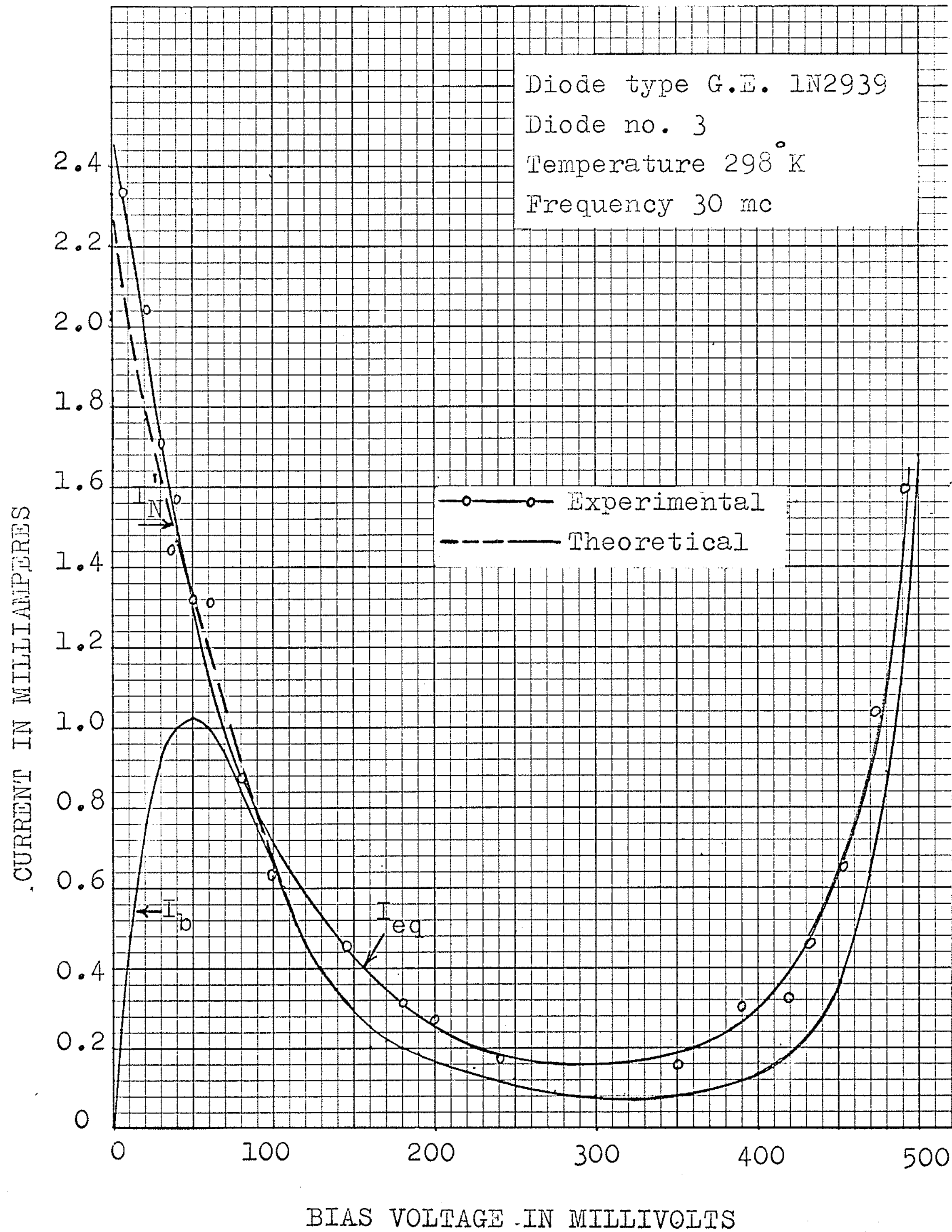

Figure 19 is a plot of I_n and $(I_{R_1} - I_{R_2})$ showing the region where a negative I_{nd} would be required.

The plot is for diode no. 3 where this effect was most evident. However, all three diodes tested exhibited this problem. The results for this method are given for only diode no. 1.

Using the Tiemann method it was possible to measure I_{eq} for all bias regions. Also considerable less soldering was required which lessened the chances of accidentally heating a component appreciably above room temperature. A minor disadvantage to this method is that the preamp must be linear. At the low signal levels involved this is almost always the case.

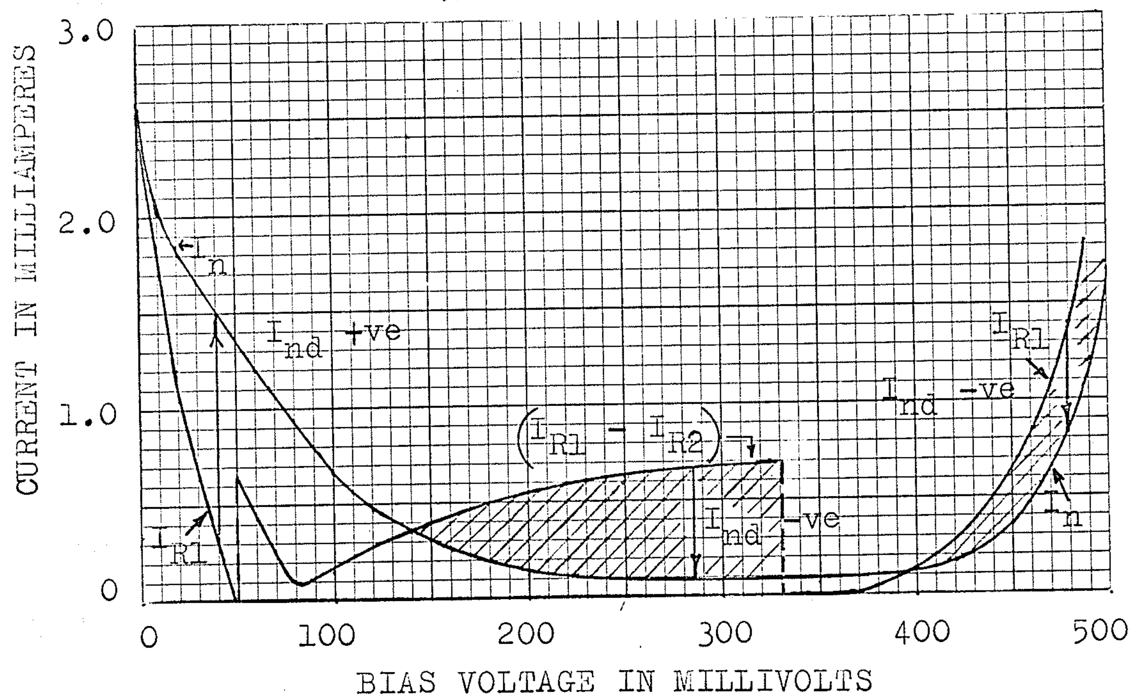

Figure 19 PLOT OF NOISE CURRENTS IN WIENS METHOD

A disadvantage of both methods used is that for portions of the characteristic where R_d is low, such as at zero bias, the receiver noise figure is very poor. The receiving system specifications give it a noise figure of 2.6db at an input impedance of 200 ohms. The receiver noise figure measurements of Appendix B show that this figure is considerably exceeded at low input impedances.

The results of the two methods agreed fairly closely in regions where a comparison could be made. The results are shown in Figure 16.

CHAPTER VII

DISCUSSION AND CONCLUSIONS

Discussion of Results

The comparison bewteen the theoretical and experimental noise currents for three G.E. type 1N2939 tunnel diodes are given in Figures 16, 17, and 18.

In the first positive conductance region I_n' and I_{eq} are in fairly good agreement for all three diodes. In each case however, I_{eq} is slightly higher than I_n'. This agrees with published results[2,5,6]. I_{eq} was difficult to measure at zero bias because resistors of fixed value were used.

In the negative conductance region I_{eq} exceeded I_n' by a considerable amount. At the valley point I_{eq} was twice I_n' for all diodes. This also agrees with results obtained by others[4,5,6]. The difference in the valley region between I_{eq} and I_n' was not as great as reported by Wiens[2] on the same type of diode. A possible reason is that he performed the noise measurements at 50°C while measurements recorded here were performed at 25°C. It has been reported[6] that the excess noise in the valley region increases slightly with temperature. It could also be that the one diode tested by Wiens had a greater than average number of unwanted impurity states in the band gap which could lead to excess noise[3].

At biases well into the second positive conductance region the theoretical and experimental noise currents con-

verge. This agrees with published results[3,4,5,6].

In Figure 10 the tunnel diode dynamic resistance and its equivalent noise resistance are compared. The tunnel diode differs from a conventional diode in that its noise resistance is greater than its dynamic resistance for a portion of its V-I characteristic. In the bias region where the tunnel diode acts as a conventional diode the reverse is true.

Application of Results to Tunnel Diode Amplifier Noise Figures

Investigations[3,17,18] of tunnel diode amplifiers show that the minimum amplifier noise figure (F_{min}) possible for a particular tunnel diode is given by:

$$F_{min} = 1 + eI_{eq}R_d/2kT_s \quad \text{.......} 7.1$$

where T_s is the source resistance temperature in degrees Kelvin. Hence for minimum noise figure the diode should be biased at a point where the product $I_{eq}R_d$ is a minimum. Figure 20 is a plot of this product for the three diodes tested.

From Figure 20 we note that this minimum occurs slightly past the point of maximum negative conductance where the diode would be biased for a maximum linear operation. For a 1N2939 the minimum $I_{eq}R_d$ is about 75 millivolts. Substituting this value in equation 7.1 gives a minimum noise figure of 2.5 or 4db for an amplifier using this particular type of diode.

FIGURE 20 MINIMUM NOISE FIGURE OF TUNNEL DIODE AMPLIFIER

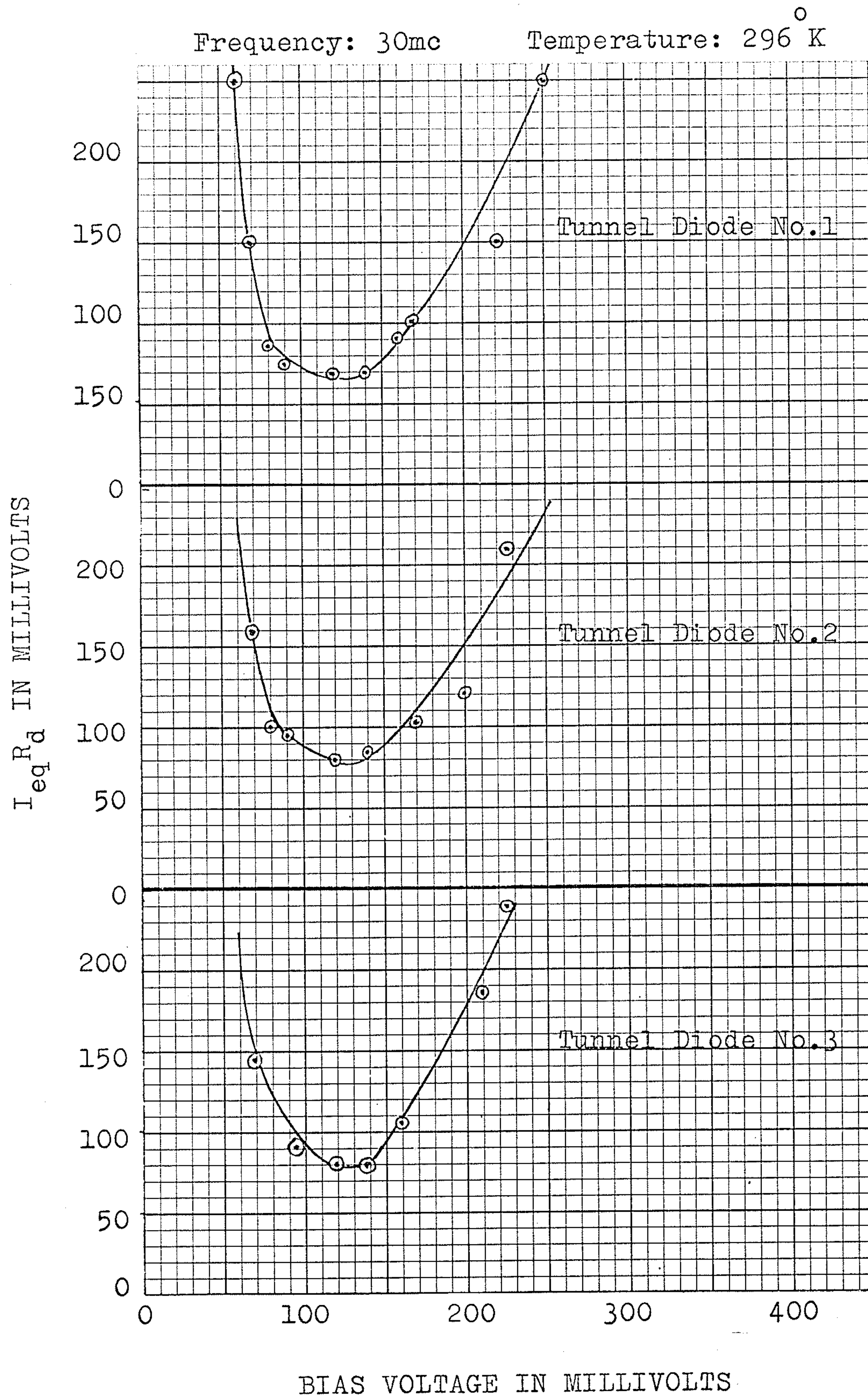

A further application of this thesis could be the design and testing of a tunnel diode amplifier using a G.E. 1N2939 tunnel diode.

Conclusions

On the basis of the results obtained the following conclusions can be made:

1. The two tunneling currents I_E and I_Z can be considered to exhibit full shot noise.

2. The excess current I_x exhibits considerably more than shot noise and cannot be considered as the result of random events.

3. The conventional diode forward current I_f exhibits full shot noise.

4. The equivalent noise resistance of a tunnel diode differs from that of conventional diodes in that it is greater than the diode's dynamic resistance for a portion of the V-I characteristic.

5. The minimum noise figure of a simple amplifier using a G.E. 1N2939 tunnel diode is about 4db. The bias point used for this optimum noise performance is slightly greater than that used for maximum linear operation.

APPENDIXES

APPENDIX A

MEASUREMENT OF TUNNEL DIODE PARAMETERS

In order to calculate the tunnel diode theoretical equivalent shot noise current I_n and the effect of the diode's parasitic elements on it, accurate knowledge of the diode's V-I characteristic, dynamic conductance, series resistance, junction capacitance and lead inductance are required. The measurement techniques used to obtain them are given below.

I MEASUREMENT OF DIODE V-I CHARACTERISTIC

Two methods of obtaining the V-I curve were used. One was an accurate point by point method, the other a visual display of the curve on an oscilloscope.

Accurate Point by Point Method

The test circuit used in this method is shown in Figure A.1.

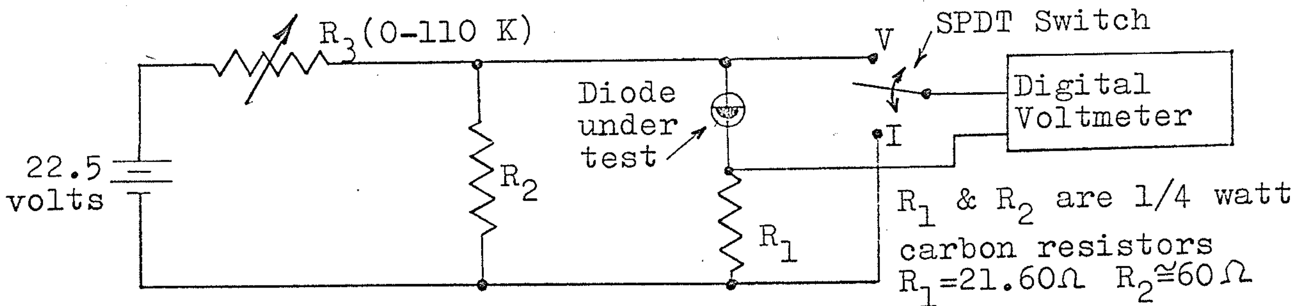

Figure A.1 CIRCUIT FOR ACCURATE MEASUREMENT OF V-I CURVE

The current sampling resistor R_1 was known to 0.1%. The four digits read on the voltmeter were all significant at full scale readings of from 10 volts to 10 millivolts. This permitted a very accurate measurements of the V-I curve.

For diode stability[19] the resistors R_1, R_2 and the total inductance L_t seen by the diode must obey the following relations:

1. $(R_1 + R_2) < |-R_d|_{min.} \cong 100$ for a 1N2939 diode.
2. $L_t < (R_1 + R_2)(|-R_d|_{min.})C_d \cong 100$ nh for a 1N2939 diode.

All diodes tested were stable in the circuit of Figure A.1.

Since the V-I curve is quite sensitive to temperature[21], care was taken to perform the noise measurements at about the same room temperature ($\pm 1^{\circ}$C) at which the V-I curve was obtained.

The curves obtained for the three G.E. 1N2939 tunnel diodes tested are given in Figures A.2, A.3, and A.4.

Oscilloscope Display of V-I Curve

During the early part of the experimental work it was apparent that some method of obtaining a quick check of the V-I curve was required. Any change in the curve due to accidental overheating while soldering could then easily be spotted. Conventional curvetracers could not be used because their large source resistance violates the stability criterion.

After considerable testing a modification of the circuit developed by Carlson[20] was adopted. The circuit is shown in Figure A.5.a. The resulting V-I curve for one of the diodes

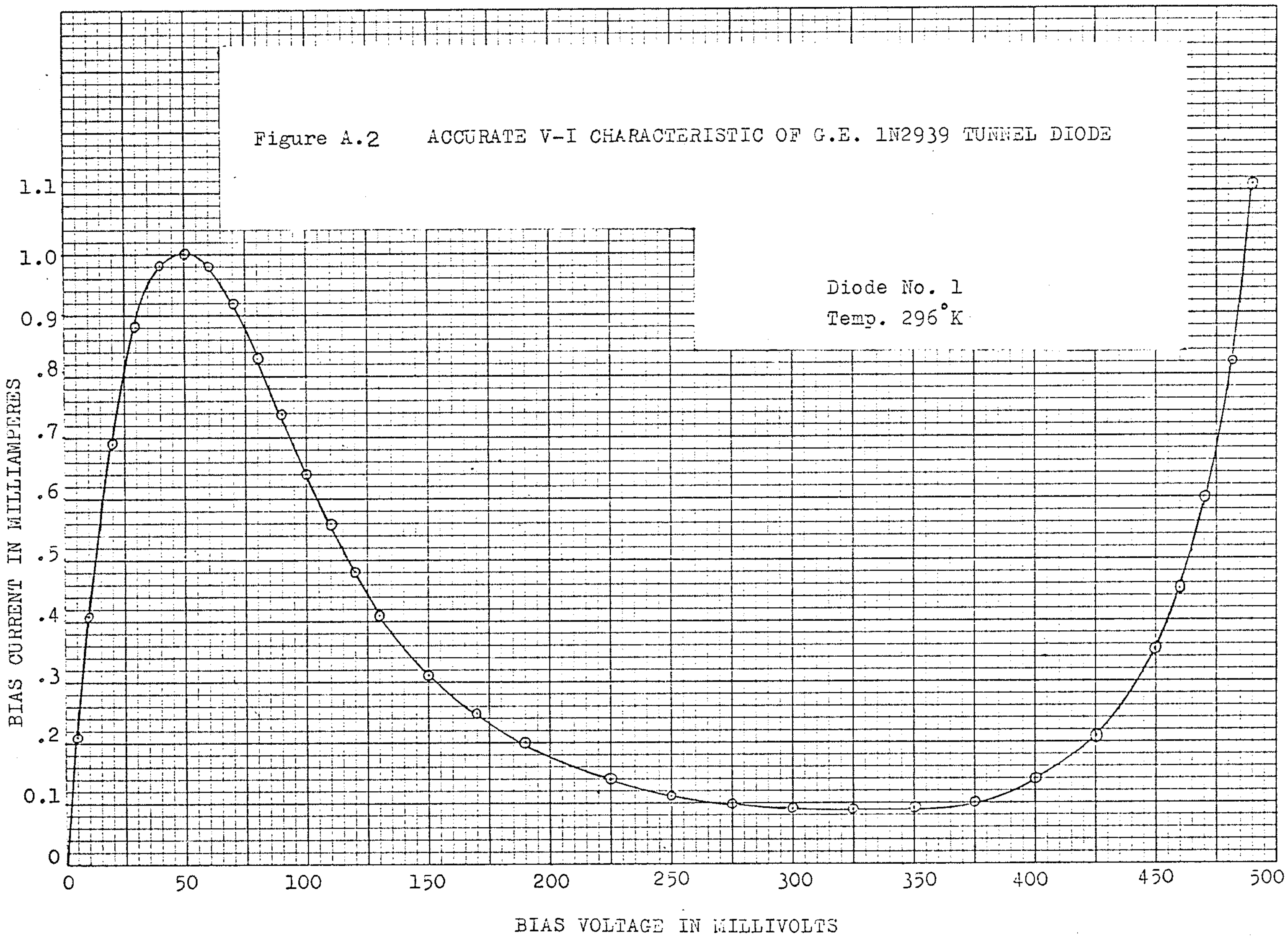

Figure A.2 ACCURATE V-I CHARACTERISTIC OF G.E. 1N2939 TUNNEL DIODE

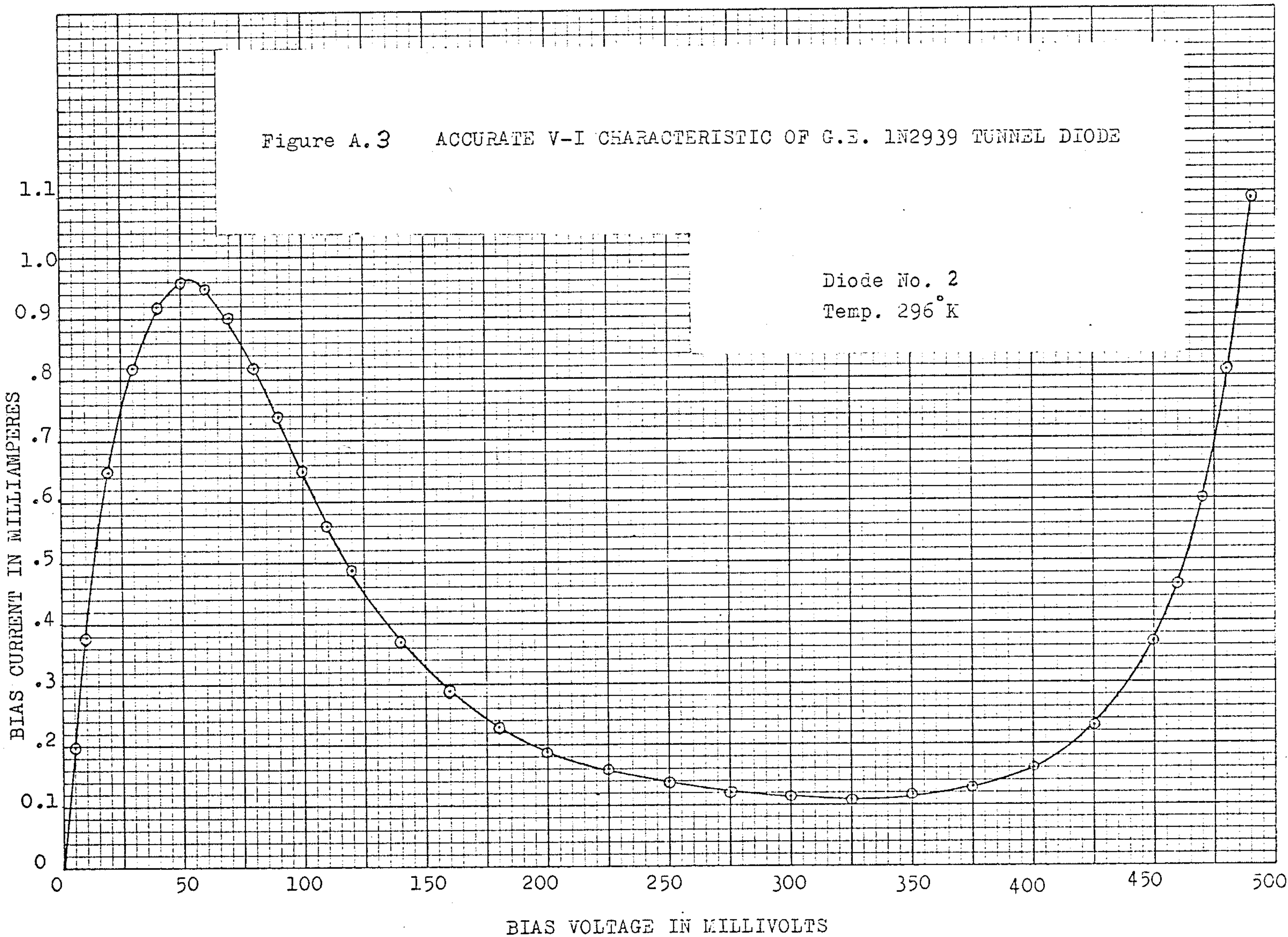

Figure A.3 ACCURATE V-I CHARACTERISTIC OF G.E. 1N2939 TUNNEL DIODE

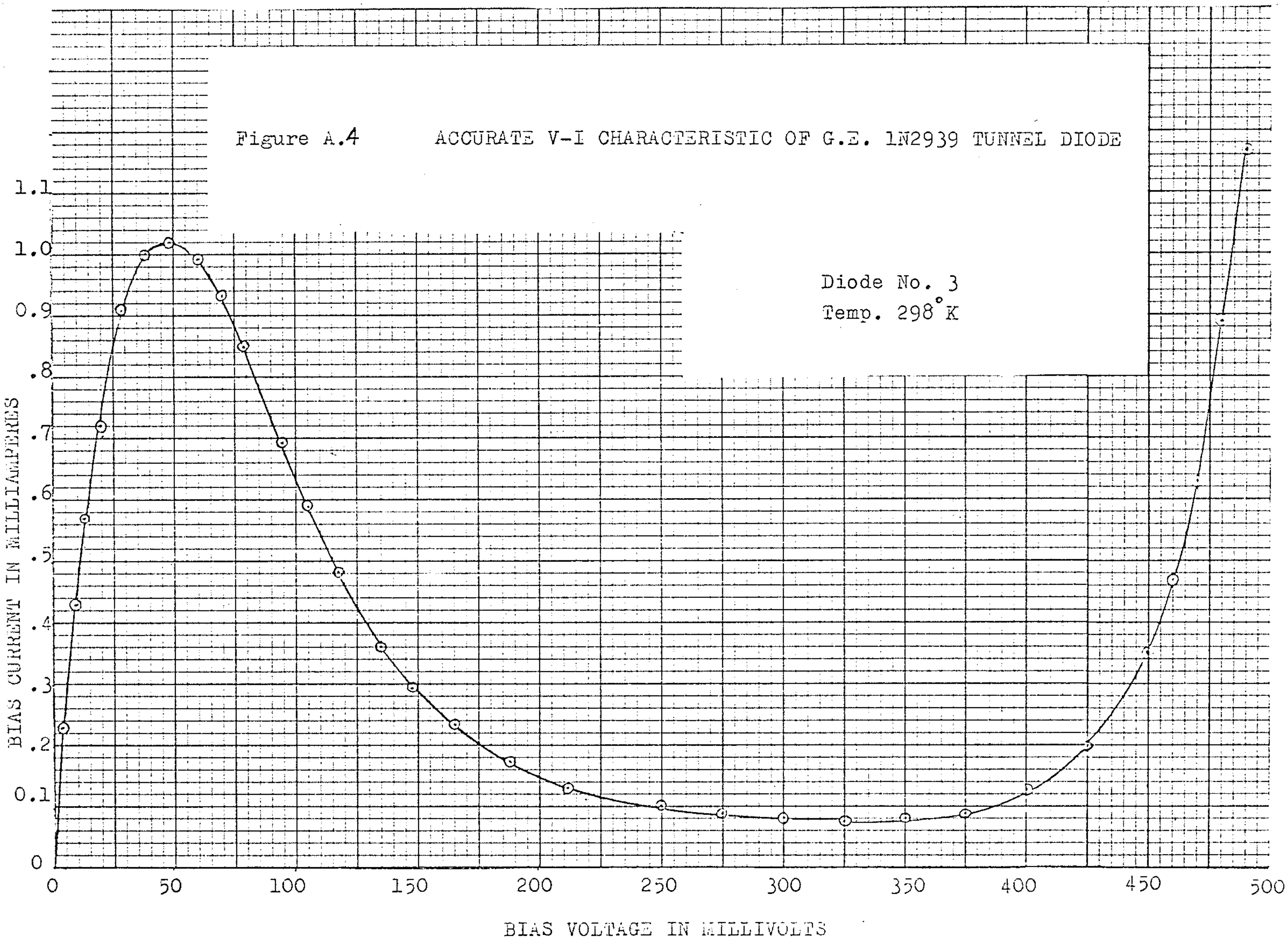

Figure A.4 ACCURATE V-I CHARACTERISTIC OF G.E. 1N2939 TUNNEL DIODE

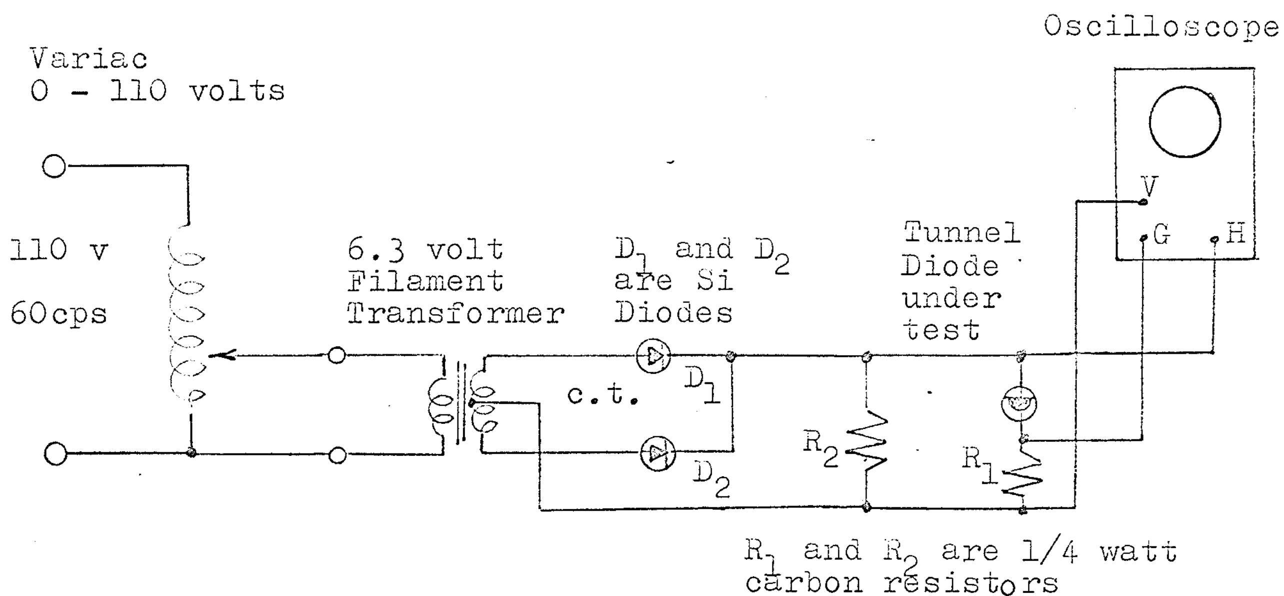

Figure A.5.a CIRCUIT FOR DISPLAYING TUNNEL DIODE V-I CURVE

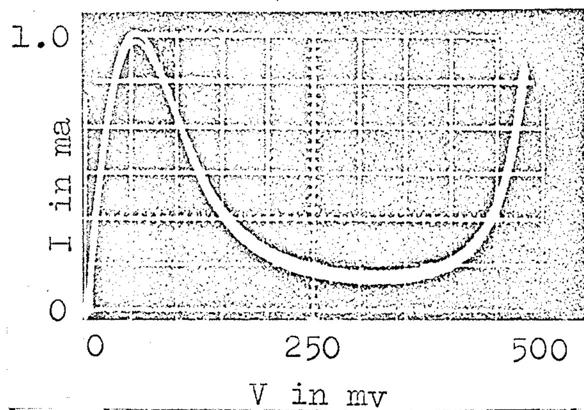

Figure A.5.b SCOPE TRACE OF STABLE DIODE V-I CURVE

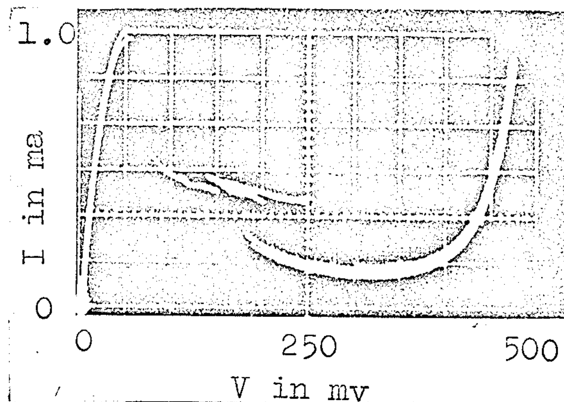

Figure A.5.c SCOPE TRACE OF V-I CURVE OF DIODE OSCILLATING DUE TO SERIES INDUCTANCE

tested is given in Figure A.5.b.

Since the diode peak current was accurately known, the vertical current scale was calibrated by adjusting the vertical gain until the peak was read on a suitable scale. The current sampling resistor therefore did not have to be accurately known.

The circuit was also used to see what values of the stabilizing resistor could be used to insure that the diode would be completely stable. Any instability could easily be spotted as shown in Figure A.5.c.

II MEASUREMENT OF DIODE DYNAMIC CONDUCTANCE

The input conductance to the equivalent circuit of Figure 11 is given by:

$$G_t = (R_d + R_s)^{-1} \quad \text{A.1}$$

if the frequency of measurement is less than $(20\ R_d\ C_d)^{-1}$ or $R_d(20\ L_s)^{-1}$. For a type 1N2939 tunnel diode the frequency must be less than 10 megacycles.

All measurements were performed at 5 megacycles using the test circuit shown in Figure A.6. The admittance bridge used was a Wayne Kerr type B801. This bridge has a conductance range of from 0 to 100 millimhos with an accuracy of $\mp 2\%$.

It was not possible to perform conductance measurements in the maximum negative conductance region due to the low resistance, high inductance path between the bridge terminals. In this region the conductance was measured by taking the slope of the accurate V-I characteristic. This method was also used by King and Sharpe[6].

Agreement between the slope and bridge method was good in the positive conductance region.

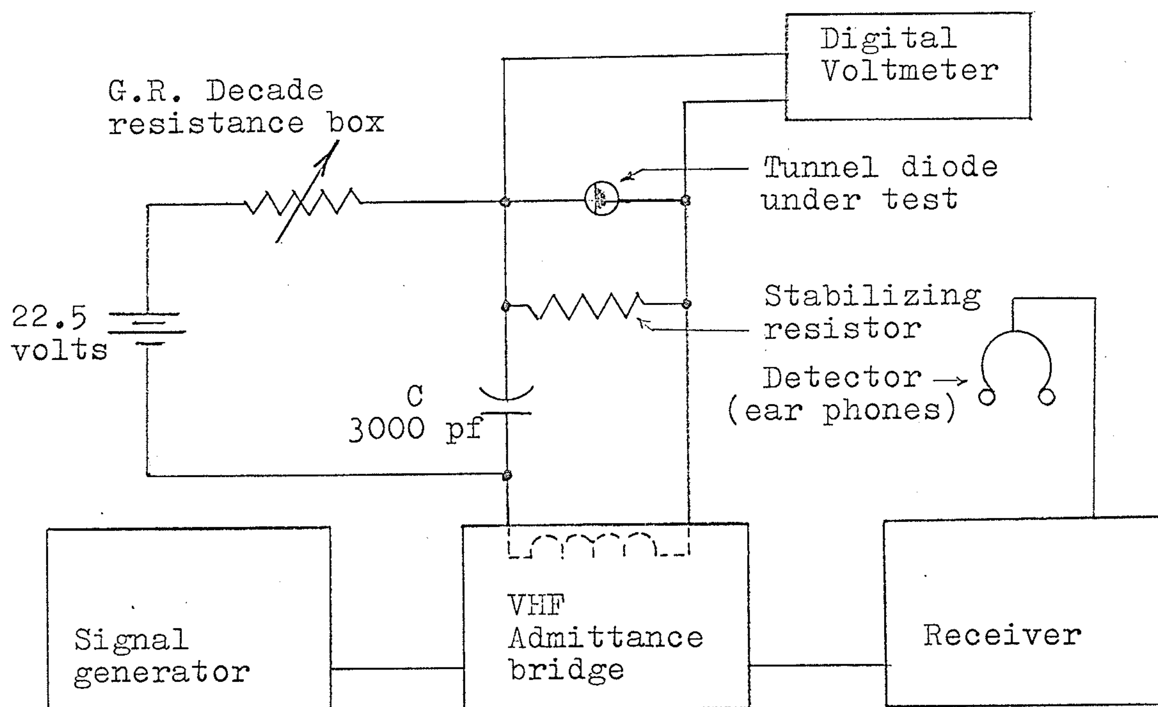

Figure A.6 TEST CIRCUIT FOR MEASUREMENT OF TUNNEL DIODE DYNAMIC CONDUCTANCE AND JUNCTION CAPACITANCE

III MEASUREMENT OF DIODE SPREADING RESISTANCE

To obtain an accurate measurement of R_s it is necessary to measure the diode resistance when it is biased in its ohmic region ($R_d = 0$). This, however, would require a bias current many times greater than that allowed by burnout considerations.

A method which overcomes this difficulty is to apply a series of low duty cycle pulses to the diode, which at their peak would bias the diode well into its ohmic region. These pulses would have a low rms value and hence burnout would not occur. An oscilloscope display of diode current versus diode voltage would give the V-I curve into the diode's ohmic region. The slope of this curve would be due to the diode's spreading and contact resistance R_s.

The circuit used for this method is as shown in Figure A.5.a. The diode connections were reversed because the ohmic region occurs at lower biases in the reverse direction. The pulses used are shown in Figure A.7.c. Using this method it was possible to attain a reverse bias current of 80 milliamperes without damaging the diode. A typical reverse characteristic obtained by this method is given in Figure A.7.a.

At the high bias currents attained the tail end of the curve is linear since R_s is constant. R_s was measured by enlarging this portion and comparing the slope with that produced by a known resistance. This procedure is shown in Figure A.7.b.

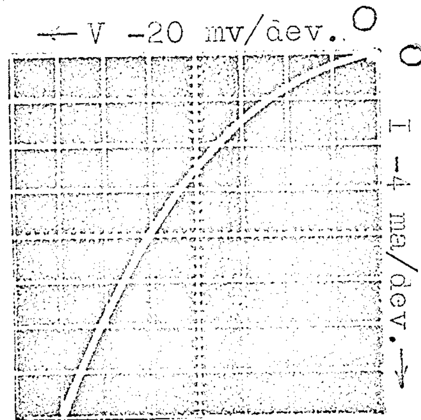

Figure A.7(a) SCOPE TRACE OF TUNNEL DIODE REVERSE V-I CHARACTERISTIC

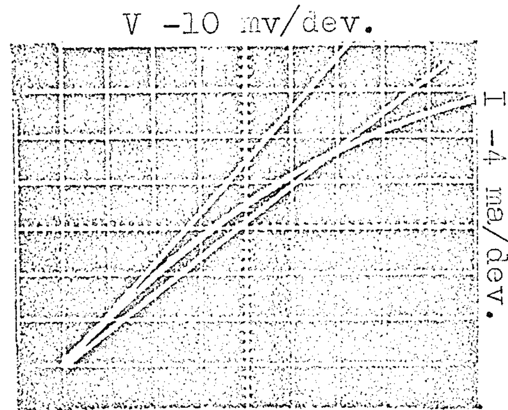

Figure A.7(b) END OF V-I CURVE WITH TWO AND THREE OHM CALIBRATION LINES

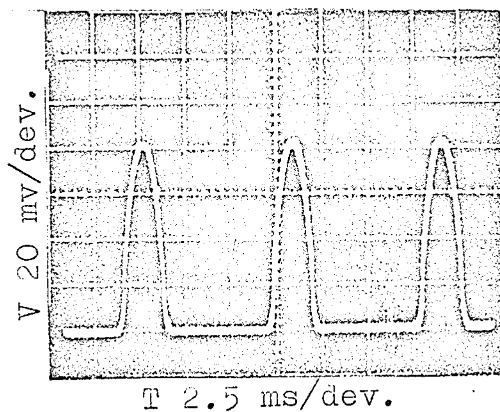

Figure A.7(c) LOW DUTY CYCLE VOLTAGE APPLIED TO DIODE FOR OBTAINING LARGE REVERSE CURRENT WITHOUT BURNOUT

The results obtained are given below.

Diode no.	1	2	3
R_s in ohms	2.5	2.3	2.0

IV MEASUREMENT OF DIODE JUNCTION CAPACITANCE

An analysis of the equivalent circuit of Figure 11 shows the total diode input capacitance to be given by:

$$C_t = C_d - L_s/R_d^2 \quad \text{.......................................A.2}$$

for the same restrictions on the frequency as in equation A.1 and the added condition that R_s is negligible compared to R_d.

If the diode is biased at the peak or valley regions, then R_d is very large and the contribution to C_t from the lead inductance is negligible. The measured input capacitance is equal to C_d. The results obtained for the three diodes tested are given below.

Diode no.	1	2	3
C_d at V_p in pf.	7	6.5	7.5
C_d at V_v in pf.	9	8	10

The test circuit used in this measurement is the same as that used to measure the diode's dynamic conductance given in Figure A.6. The Wayne Kerr admittance bridge used has a capacitance range of 0 to 230 pf with an accuracy of $\mp 2\%$.

V MEASUREMENT OF DIODE LEAD INDUCTANCE

A precise direct measurement of L_s is very difficult to make and requires elaborate test equipment[21].

A simpler method of determining L_s is apparent from equation A.2. If a capacitance measurement is made at biases where R_d is small (at zero bias) the inductance effect will predominate and C_t will be negative. L_s can then be calculated from:

$$L_s = C_d R_d - C_t(R_d + R_s) \qquad \text{A.3}$$

The results obtained are given below.

Diode no.	1	2	3
L_s in nh.	43	39	35

APPENDIX B

MEASUREMENT OF RECEIVER NOISE FIGURE

During the noise measurements outlined in Chapter 6, the receiver preamplifier is subjected to a wide range of input terminations. To see how this affects the noise performance of the receiving system, its noise figure was measured for the different input terminations used.

The IRE Standards on methods of measuring noise in linear twoports[22] defines the noise figure F at a specified frequency as the ratio of 1) the total noise power per unit bandwidth at a corresponding output frequency available at the output port when the noise temperature of the input termination is standard (290°K) to 2) that portion of 1 engendered at the input frequency by the input termination. As defined, F depends only on the internal structure of the receiver and on its input termination.

When dealing with a receiver where the input signal is distributed over a finite bandwidth, it is more convenient to talk of an average noise figure $\overline{F}$. The average noise figure is the weighted average of F over the band in question, the weighting factor being the receiver gain.

The relationship between $\overline{F}$ and F is given by:

$$\overline{F} = \frac{\int F(f)G(f)\, df}{\int G(f)\, df}$$

The method used to measure $\bar{F}$ was as given in the IRE Standards on Noise Measurements in Linear Twoports[22]. The test circuit used is as given in Figure 15.

With the input termination in question in terminals x-x, and the noise generator output zero, an output reading of I_1 was obtained on the output meter. The preamplifier gain was kept full up during all parts of the test so that the noise produced by it would swamp any noise in the precision receiver.

Three db of attenuation were then placed in the circuit and noise added from the noise generator until an output reading of I_1 was again obtained. The plate current of the noise diode I_{nd} was recorded. The noise power added from the noise generator P_{nd} was now equal to the noise power from the input termination P_{Ri} plus the noise added by the preamplifier.

From the definition of $\bar{F}$ it is seen that:

$$\bar{F} = \frac{P_{nd}}{P_{Ri}} \qquad \text{A.4}$$

The noise power output due to the noise generator is given by:

$$P_{nd} = 2eI_{nd}BG \qquad \text{A.5}$$

where G is the receiver gain when the input termination is Ri.

The noise power output due to the input termination is given by:

$$P_{Ri} = 4kTBG/Ri \quad \text{A.6}$$

Combining equations A.4, A.5, and A.6 gives:

$$\bar{F} = eI_{nd}Ri/2kT \quad \text{A.7}$$

A plot of $\bar{F}$ for different values of Ri are given in Figure A.8.

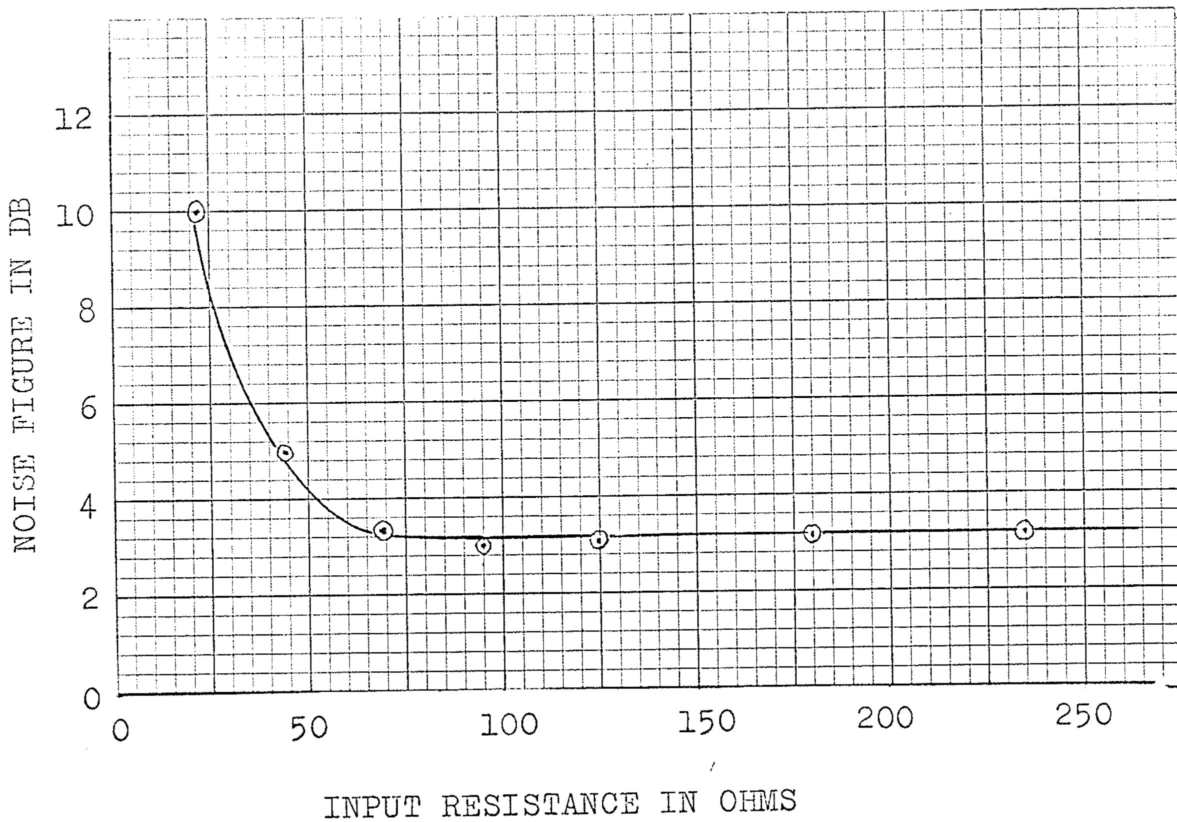

FIGURE A.8 RECEIVER NOISE FIGURE

BIBLIOGRAPHY

1. L. Esaki. New Phenomenon in Narrow Germanium P-N Junctions, Phys. Rev., Vol. 109, p. 603; Jan.-Mar., 1958.

2. J. Wiens. Noise Characteristics of Tunnel Diodes, M.Sc. Thesis, University of Manitoba; Feb., 1963.

3. R.R.N. Chang. Low Noise Tunnel Diode Amplifier, Proc. IRE, Vol. 47, p. 1268; July, 1959.

4. J.J. Tiemann. Shot Noise in Tunnel Diode Amplifiers, Proc. IRE, Vol. 48, p. 1418; Aug., 1960.

5. D.C. Agouridis, K.M. van Vliet. Noise Measurements on Tunnel Diodes, Proc. IRE, Vol. 50, p. 2121; Oct., 1962.

6. B.G. King, O.E. Sharpe. Measurement of the Spot Noise of Germanium, Gallium Antimonide, Gallium Arsenide and Silicon Esaki Diodes, IEEE Trans. on Elect. Dev., p. 273; 1964.

7. R. Hall. Tunnel Diodes, IRE Trans. on Elect. Dev., p. 1; Jan., 1960.

8. R. Nanavati. An Introduction to Semiconductor Electronics, McGraw-Hill, 1963. (a) p. 370

9. A.G. Chynoweth, W.L. Feldmann, R.A. Logan. Excess Tunnel Current in Silicon Esaki Junctions, Phys. Rev., Vol. 121 No. 3, p. 684; Feb., 1961.

10. C.B. Pierce, H.H. Sander, A.D. Kantz. Radiation Induced Hump Structure in the I-V Characteristic of Esaki Diodes, J. of Applied Phys., Vol. 33, p. 33108; Oct., 1962.

11. J.B. Johnson. Thermal Agitation of Electricity in Conductors, Phys. Rev., Vol. 32, p. 97; 1928.

12. H. Nyquist. Thermal Agitation of Electrical Charge in Conductors, Phys. Rev., Vol. 32, p. 110; 1928.

13. C.J. Christenson, G.L. Pearson. Spontaneous Resistance Fluctuations in Carbon Microphones and Other Granular Resistances, Bell Sys. Tech. J., Vol. 15, p. 197; 1936.

14. A. van der Ziel. Noise, Prentice-Hall, 1954. (a) p. 213 (b) p. 209

15. W.R. Bennet, Electrical Noise, McGraw-Hill, 1960. (a) p.82; (b) p.91.

16. R.H. Mattson, A. van der Ziel. Shot Noise in Germanium Filaments, J. of Applied Phys., Vol.24, p.222; 1953.

17. A. Yariv, J.S. Cook. A Noise Investigation of Tunnel Diode Microwave Amplifiers, Proc. IRE, Vol.49, p.739; April 1961.

18. E.G. Neilsen. Noise Performance of Tunnel Diodes, Proc. IRE, Vol.48, p.1903; Nov. 1960.

19. L.I. Smilen, D.C. Youla, Stability Criteria for Tunnel Diodes, Proc. IRE, Vol.49, p.1206; July 1961.

20. A.Carlson. Measurement of Tunnel Diode Parameters, Electronic Components, p.633; June 1963.

21. General Electric. Tunnel Diode Manual, First Edition, 1961.

22. IRE Standards on Methods of Measuring Noise in Linear Twoports, 1959, Proc. IRE, Vol.47, p.61; Jan. 1959.

23. M. Schwartz. Information Transmission, Modulation, and Noise, McGraw-Hill, 1959.